

DESIGNING OF ECO- FRIENDLY FOAM NET FOR GUAVA USING FINITE
ELEMENT METHOD (FEM)

THEERAPAT TAWEEBRAKSA



A Thesis Submitted in Partial Fulfillment of the Requirements for the
Degree of Master of Engineering in Materials Engineering
Suranaree University of Technology
Academic Year 2024

การออกแบบตาข่ายโฟมเป็นมิตรกับสิ่งแวดล้อมสำหรับฝรั่งโดยใช้วิธี

ไฟไนต์เอลิเมนต์

นายธีรพัฒน์ ทวีปรักษา



วิทยานิพนธ์นี้เป็นส่วนหนึ่งของการศึกษาตามหลักสูตรปริญญาวิศวกรรมศาสตรมหาบัณฑิต

สาขาวิชาวิศวกรรมวัสดุ

มหาวิทยาลัยเทคโนโลยีสุรนารี

ปีการศึกษา 2567

DESIGNING OF ECO- FRIENDLY FOAM NET FOR GUAVA USING FINITE ELEMENT METHOD (FEM)

Suranaree University of Technology has approved this thesis submitted in partial fulfillment of the requirements for a Master's degree

Thesis Examining Committee

.....*Kasama Jarukumjorn*.....

(Assoc. Prof. Dr. Kasama Jarukumjorn))

Chairperson

.....*T. Trongsatitkul*.....

(Assoc. Prof. Dr. Tatiya Trongsatitkul)

Member (Thesis Advisor)

.....*Keerati Suluksna*.....

(Assist. Prof. Dr. Keerati Suluksna)

Member (Thesis Co-advisor)

.....*Saowapa Chaiwong*.....

(Assoc. Prof. Dr. Saowapa Chaiwong)

Member (Thesis Co-advisor)

.....*Petch Jearaaisilawong*.....

(Assoc. Prof. Dr. Petch Jearaaisilawong)

Member

.....*Pranee Chumsamrong*.....

(Assoc. Prof. Dr. Pranee Chumsamrong)

Member

.....*Veena Phunpeng*.....

(Assoc. Prof. Dr. Veena Phunpeng)

Member

.....*Pornsiri Jongkol*.....

(Assoc. Prof. Dr. Pornsiri Jongkol)

.....*Yupaporn Ruksakulpiwat*.....

(Assoc. Prof. Dr. Yupaporn Ruksakulpiwat)

Vice Rector for Academic and Affairs and
Quality Assurance

Dean of Institute of Engineering

ธีรพัฒน์ ทวีปรีक्षा : การออกแบบตาข่ายโฟมเป็นมิตรกับสิ่งแวดล้อมสำหรับฝรั่งโดยใช้วิธีไฟไนต์เอลิเมนต์ (DESIGNING OF ECO- FRIENDLY FOAM NET FOR GUAVA USING FINITE ELEMENT METHOD (FEM)).

อาจารย์ที่ปรึกษา : รองศาสตราจารย์ ดร.ตติยา ตรงสถิตกุล, 79 หน้า.

คำสำคัญ : บรรจุภัณฑ์ ประสิทธิภาพการกันกระแทก การทดสอบการตก การจำลอง ระเบียบวิธีไฟไนต์เอลิเมนต์

ตาข่ายโฟมกันกระแทกที่เป็นมิตรต่อสิ่งแวดล้อมซึ่งผลิตจากน้ำยางธรรมชาติ ได้รับการพัฒนาขึ้นเพื่อใช้เป็นส่วนประกอบป้องกันสำหรับบรรจุภัณฑ์ผลิตผลสดเพื่อแก้ไขปัญหาสิ่งแวดล้อม แม้ว่าการศึกษาก่อนหน้านี้แสดงให้เห็นว่าประสิทธิภาพการกันกระแทกของมันเป็นเทียบเท่ากับตาข่ายโฟมเชิงพาณิชย์ แต่ความหนาแน่นที่สูงกว่าของยางธรรมชาติเป็นความท้าทายที่สำคัญสำหรับการใช้งานจริง งานวิจัยนี้มีเป้าหมายเพื่อเพิ่มประสิทธิภาพของบรรจุภัณฑ์โฟม ในขณะที่ยังคงรักษาความสามารถในการป้องกันไว้ วัตถุประสงค์หลักคือการศึกษาว่าตัวแปรโครงสร้างความหนาแน่นของโฟม จำนวนเส้นใย และเส้นผ่านศูนย์กลางของเส้นใย ที่ส่งผลต่อประสิทธิภาพการกันกระแทก โดยใช้การวิเคราะห์โดยโปรแกรมการจำลองเพื่อลดความเสียหายทางกลต่อผลิตผลสด

ฝรั่ง กลมสาเลี (250 กรัม) ซึ่งเป็นตัวแทนของผลไม้ทรงกลมและไวต่อแรงกระแทก ได้รับการเลือกเป็นแบบจำลองสำหรับการศึกษานี้ การจำลองด้วยระเบียบวิธีไฟไนต์เอลิเมนต์ได้ดำเนินการโดยใช้แบบจำลอง คอมพิวเตอร์ช่วยออกแบบ ที่สร้างขึ้นในโปรแกรม SolidWorks® และวิเคราะห์ในโปรแกรม ANSYS® โมดูลexplicit dynamics การจำลองสามชุดได้ดำเนินการเพื่อสำรวจผลกระทบของตัวแปรการออกแบบที่แตกต่างกัน: ชุดแรกเปรียบเทียบฝรั่งที่ไม่มีการป้องกัน (ไม่มีบรรจุภัณฑ์) กับโฟมทางการค้า (โฟมพอลิเอทิลีนแบบขยายหรืออีพีอีโฟม) ชุดที่สองตรวจสอบการเปลี่ยนแปลงจำนวนเส้นใย (25, 20 และ 15 เส้นใย) และเส้นผ่านศูนย์กลางของเส้นใย (2.5, 3.5 และ 4.5 มิลลิเมตร.) และชุดที่สามประเมินความหนาแน่นของโฟมในสามระดับ (420, 397 และ 345 กิโลกรัมต่อลูกบาศก์เมตร) ใช้ความสูงในการตก 100 และ 200 มิลลิเมตร. ขึ้นอยู่กับตัวแปรที่ศึกษา

ผลการจำลองเผยให้เห็นว่าฝรั่งที่บรรจุภัณฑ์โฟมมีระดับความเครียดทางกลสูงสุด ในขณะที่บรรจุภัณฑ์โฟมยางธรรมชาติ ที่มีจำนวนเส้นใยมากขึ้นและเส้นผ่านศูนย์กลางของเส้นใยใหญ่กว่าช่วยปรับปรุงการลดแรงกระแทกอย่างมีนัยสำคัญ ในทางตรงกันข้าม การลดความหนาแน่นของโฟมนำไปสู่ประสิทธิภาพการดูดซับแรงกระแทกที่ลดลง ความเครียดสูงสุดทางกลถูกใช้เป็นตัวชี้วัดประสิทธิภาพหลัก โดยค่าที่ต่ำกว่าบ่งบอกถึงประสิทธิผลการกันกระแทกที่ดีกว่า

สุดท้ายนี้ วิทยานิพนธ์นี้ให้ข้อมูลเชิงลึกที่เกี่ยวกับการออกแบบบรรจุภัณฑ์โพลีเอทิลีนชนิดความหนาแน่นสูง (HDPE) สำหรับบรรจุภัณฑ์อาหารประเภทผักและผลไม้สด ซึ่งมีความสำคัญต่อการพัฒนาอุตสาหกรรมบรรจุภัณฑ์ในประเทศไทย การศึกษาครั้งนี้ยังเน้นย้ำถึงอิทธิพลของการออกแบบที่สำคัญของจำนวนเส้นใย เส้นผ่านศูนย์กลางของเส้นใย และความหนาแน่นของบรรจุภัณฑ์โพลีเอทิลีนชนิดความหนาแน่นสูง ต่อประสิทธิภาพทางกลและประสิทธิภาพการดูดซับแรงกระแทกของโพลีเอทิลีนชนิดความหนาแน่นสูง ซึ่งสนับสนุนศักยภาพของมันในฐานะทางเลือกที่ยั่งยืนแทนบรรจุภัณฑ์โพลีเอทิลีนชนิดความหนาแน่นสูงสังเคราะห์



สาขาวิชาวิศวกรรมพอลิเมอร์

ปีการศึกษา 2567

ลายมือชื่อนักศึกษา

ลายมือชื่ออาจารย์ที่ปรึกษา

ลายมือชื่ออาจารย์ที่ปรึกษาร่วม

ลายมือชื่ออาจารย์ที่ปรึกษาร่วม

Theerapat Tanwattana
T. Tanwattana
Sun-ya
Keerti Aulakh

THEERAPAT TAWEEBRAKSA: DESIGNING OF ECO- FRIENDLY FOAM NET FOR GUAVA USING FINITE ELEMENT METHOD (FEM). THESIS ADVISOR: ASSOC. PROF. TATIYA TRONGSATITKUL, Ph.D., 79 PP.

Keyword: Packaging/ Cushion performance/ Drop test/ Simulation/ finite element method

An eco-friendly cushion foam net fabricated from natural rubber latex (NRL) has been developed as a protective component for fresh-produce packaging to address environmental concerns. Although previous studies demonstrated that its cushioning performance is comparable to commercial foam nets, the higher density of natural rubber presents a significant challenge for practical implementation. This research aims to use finite element simulation to optimize the weight of NRL foam cushions while maintaining their protective capabilities. The primary objective is to investigate how structural parameters foam density, filament number, and filament diameter affect cushioning performance, using simulation-based analysis to minimize mechanical damage to fresh produce.

A *Glom Sali* guava (250 g), representing a typical spherical and impact-sensitive fruit, was selected as the model for this study. Finite Element Method (FEM) simulations were performed using CAD models generated in SolidWorks® and analyzed in ANSYS® explicit dynamics. Three sets of simulations were conducted to explore the effects of different design parameters: the first compared unprotected guavas (without packaging) to those cushioned with commercial Expanded polyethylene (EPE) foam; the second examined variations in filament number (25, 20, and 15 filaments) and filament diameter (2.5, 3.5, and 4.5 mm); and the third evaluated foam density at three levels (420, 397, and 345 kg/m³). Drop heights of 100 mm and 200 mm were used depending on the variable under study.

Simulation results revealed that guavas without cushioning experienced the highest stress levels, while natural rubber latex foam (NRLF) cushions with higher filament numbers and larger filament diameters significantly improved impact mitigation. In

contrast, reductions in foam density led to decreased shock-absorbing performance. Maximum stress was used as the primary performance indicator, with lower values indicating better cushioning effectiveness.

Finally, this thesis provides valuable insight into the design of environmentally friendly impact-absorbing foam packaging using computer-aided design and FEM simulations. This approach offers faster and more efficient analysis than traditional experimental methods. Furthermore, the study highlights the significant influence of filament number, filament diameter, and foam density on the mechanical performance and impact absorption efficiency of NRLF cushions, supporting their potential as a sustainable alternative to synthetic foam packaging.



School of Polymer Engineering
Academic Year 2024

Student's Signature

Advisor's Signature

Co-Advisor's Signature

Co-Advisor's Signature

Theerapat Taveedee
T. Taveedee
S. S.
Keerti Aulakh

ACKNOWLEDGMENTS

I would like to express my deepest gratitude to Associate Professor Dr. Tatiya Trongsatitkul, my main advisor, for imparting knowledge and guiding me to deeply understand engineering polymers, as well as for being a constant source of inspiration throughout my academic journey.

I also extend my sincere thanks to Assistant Professor Dr. Keerati Sulaksna (School of Mechanical Engineering, Suranaree University of Technology), my co-advisor, who introduced me to and ignited my passion for Computer-Aided Engineering (CAE) and has been a crucial driving force in my engineering path.

Special appreciation is extended to Associate Professor Dr. Saowapa Chaiwong (School of Agro-Industry, Mae Fah Luang University) for her invaluable advice and generous support throughout my research journey.

I am deeply grateful to Suranaree University of Technology and Mae Fah Luang University for providing facilities, equipment, and academic opportunities, as well as to The KING PRAJADHIOP and QUEEN RAMBHAJI BARNI Memorial Foundation and the Rubber Authority of Thailand for their financial support that made this research possible.

Moreover, I am grateful for my trusty computers WUAWEL D15 Ryzen 7 3700U and Dell Latitude 7340 operating on an x86 system, for their tireless performance throughout countless simulations.

Finally, I sincerely thank myself for the perseverance, endurance, dedication, and faith that carried me forward, even when the road seemed impossible, and the journey was at its most challenging.

Theerapat Taweabraks

TABLE OF CONTENTS

	Page
ACKNOWLEDGMENTS	v
TABLE OF CONTENTS	vi
LIST OF TABLES	x
LIST OF FIGURES	ix
CHAPTER	
I. INTRODUCTION	ix
1.1 Background and problem	1
1.2 Research objectives	1
1.3 Goals	2
1.4 Scope and limitations	3
1.4.1. Limitations of the study	3
1.5 Research benefits	4
II. LITERATURE REVIEW	6
2.1 Introduction	6
2.2 Transportation damage	6
2.3 Impact damage	7
2.4 Impact damage to fresh produce	7
2.4.1. Package cushioning	8
2.5 Finite element method	9

TABLE OF CONTENTS(Continued)

	Page
2.5.1. Differential equation	10
2.6 FEM for solid mechanics problems.....	10
2.6.1. Surface traction.....	11
2.6.2. Three-dimensional isoperimetric elements.	14
2.7 Mesh generation.....	14
2.8 Failure theories of material.....	15
2.8.1. Brittle fracture	16
2.8.2. Ductile fracture	16
2.8.3. Triaxial stress	17
2.8.4. Von-Mises yield criteria.	19
III. METHODOLOGY	21
3.1 Material	21
3.1.1. NRL Foam.....	21
3.1.2. Cushioning materials and testing	23
3.1.3. Testing Method.....	23
3.1.4. Mechanical Characterization of Guava.....	27
3.1.5. Characterization of Mechanical Properties.....	27
3.1.6. Poisson's ratio.....	30
3.2 Computer-aided design	34
3.3 Finite element analysis	34
3.3.1. Model Analysis.....	34

TABLE OF CONTENTS(Continued)

	Page
3.3.2. Preprocess.....	35
3.4 Validation.....	45
3.4.1. Boundary Conditions Setting for Validation	47
IV. RESULTS AND DISCUSSION.....	51
4.1 Introduction.....	51
4.2 Parameter variation and result.....	51
4.3 Effect of size and number on cushion performance.....	55
4.4 Density Reduction Effects on Impact Protection.....	63
V. CONCLUSIONS.....	73
5.1 Conclusion.....	73
5.2 Suggestions.....	75
REFERENCES.....	77
BIOGRAPHY.....	79

LIST OF TABLES

Table	Page
3.1. Formulation of the natural rubber latex (NRL) compounds for the synthesis of reinforcing NRL foam (NRLF).....	21
3.2 Compressive stress at 50% Strain of foam samples	26
3.3 Mechanical properties of foam samples and guava	33
3.4 Direction of setting standard earth gravity	40
3.5 Material parameters	40
3.6 Mesh method and element size	42
3.7 Mesh convergence	45
3.8 Material properties for the drop test simulation analysis	48
3.9 Comparison of experimental and simulated bruise areas	49
4.1 Relationship between number of filaments, density, and weight	72

LIST OF FIGURES

Figure	Page
2.1 The process of computer aid designs and numerical techniques	9
2.2 Workflow of pre-processing FEM simulation.....	9
2.3 Triaxial Stress State (James Gere, 2008.).....	11
2.4 The traction vector (T), (stress vector at the point) on the surface surrounding the point with normal vector \mathbf{n} is defined as.....	12
2.5 Rigid body equilibrium 3D.....	13
2.6 Finite element mesh of quadrilaterals of a curved domain.	15
2.7 Mesh generation	15
2.8 Stress-strain curves of brittle material, ductile material-compression test.....	16
2.9 Diagram failure theories of material.....	17
2.10 Triaxial stress state mechanics of materials (James Gere, 2008).....	17
2.11 failure envelope as per maximum shear stress theory.....	19
2.12 Comparison of the yield locus for the plane stress of von Mises yield criterion and Tresca yield criterion.	20
3.1 Flowchart of processing step NRL foam	22
3.2 Sample cube specimen of 50 mm X 50 mm X 25 mm used in the study.....	24
3.3 Universal testing machine (INSTRON/5565, Norwood, MA, USA).	25
3.4 Stress-strain curve of the EPE and NRLF foam obtained using a compression test.	25
3.5 Sample cube specimen of 50 mm X 50 mm X 25 mm follower ASTM D3574 test C under compression testing.	26
3.6 Stress-strain curve of the EPE foam obtained using a compression test.....	26

LIST OF FIGURES(Continued)

Figure	Page
3.7 (a) Guava fruit (<i>Psidium guajava</i> L.) cv. Glom Sali (b) Sample cube specimen of guava (<i>Psidium guajava</i> L.) using in the present study sample size 20 mm x 20 mm.	28
3.8 Stress-strain curve of the Guava (<i>Psidium guajava</i> L.) obtained using a compression test.	30
3.9 The Poisson's ratio of a material.....	30
3.10 A cube made of an isotropic linearly elastic material is stretched along	31
3.11 Schematic explanation of the two-dimensional poisson effect	31
3.12 Sample cube specimen of guava (<i>Psidium guajava</i> L.) using in the present study sample size 20 mm x 20 mm.	32
3.13 Determine of NRLF negative Poisson's ratio using UTM.	32
3.14 Force displacement curve of Guava fruit (<i>Psidium guajava</i> L.) Glom Sali	33
3.15 Flow chart of CAD/CAE design analysis (Chang. 2013).....	34
3.16 Guava with commercial expanded polyethylene foam net CAD Modeling NRLF net foam cushion.....	35
3.17 CAD cushion foam net 20 mesh filament number on NRLF 3.5 mm	36
3.18 CAD model guava with expanded polyethylene cushion foam net	36
3.19 Simplifications of simulation model.....	37
3.20 3D model of commercial cushion foam net	38
3.21 CAD 3D model filament dimension 3.5 mm (number a:25, b: 20, and c: 15 filament).....	38
3.22 FEM model for simulating with the impact plane drop test.....	39
3.23 FEM model boundary conditions drop high setting	40

LIST OF FIGURES(Continued)

Figure	Page
3.24 Finite element model (a) reverse-engineered guava cushion foam net model, outer mesh structure, (b) inner mesh structure)	41
3.25 Show cross section in meshing setup of EPE cushion net foam 3.5X25 mm and guava mesh size 3.00mm	42
3.26 Effect of mesh size, Nodes, and elements on CAD model of NRLF cushion net foam 3.5 mm 25x25.....	43
3.27 Mesh sensitivity analysis	44
3.28 The experimental fruit bruise damage.....	47
3.29 Validation model using FEM Drop test simulation setup.....	48
4.1 Stress [MPa] in the gravity direction for the drop height 200 mm model (a) guava unpacking (b) guava with EPE commercial cushion	53
4.2 Maximum von-miss equivalent stress of guava and time at 0.016 s. drop height of 200 mm.	54
4.3 Maximum (von-miss) drop test of guava bear fruit compared to EPE commercial cushion foam net.	54
4.4 Stress in the gravity direction for the drop height model (a) NRLF 2.5x15, (b) NRLF 2.5x20 and (c) NRLF 2.5x25 from a cross-section view.....	56
4.5 Stress distribution plots in guava sample (max von-mises stress, [MPa]) of NRLF foam net diameter filament size 2.5 mm.	57
4.6 Stress [MPa] in the gravity direction for the drop height model (a) NRLF 3.5x15, (b) NRLF 3.5x20 and (c) NRLF 3.5x15 from a cross-section view show at time 0.0012 s.....	58
4.7 Stress distribution plots in guava sample (max von-mises stress, [MPa]) of NRLF foam net diameter filament size 3.5 mm.	59

LIST OF FIGURES(Continued)

Figure	Page
4.8 Stress [MPa] in the gravity direction for the drop height model (a) NRLF 4.5x15, (b) NRLF 4.5x20 and (c) NRLF 4.5x15 from a cross-section view show at time 0.0012 s.....	60
4.9 Stress distribution plots in guava sample (max von-mises stress, [MPa]) of NRLF foam net diameter filament size 4.5 mm.	61
4.10 Maximum (von-miss) drop test of Guava NRLF packaging.....	61
4.11 Maximum equivalent stress drop test 200 mm was observed at 0.013 s after impact and NRLF filament number 25....	62
Figure 4.12 Maximum equivalent stress drop test 200 mm was observed at 0.013 s after impact of bear fruit and EPE...	63
4.13 Stress [MPa] in the gravity direction for the drop height 100 mm filaments number 25 and the density (kg/m^3) (a) 420, and (b) 397 from a cross-section view.	65
4.14 Stress [MPa] in the gravity direction for the drop height 100 mm filaments number 25 and the density (kg/m^3) (a) 420, (b) 397, and (c) 345 from a cross-section view.....	66
4.15 Plot Maximum stress (MPa) Time (s) plot for the model of filaments number 25 of and the density (kg/m^3) 420, 397, and 345.....	66
4.16 Stress in the gravity direction for the drop height 100 mm filaments number 20 and the density (kg/m^3) (a) 420, and (b) 397 from a cross-section view.	67
4.17 Stress in the gravity direction for the drop height 100 mm filaments number 20 and the density (kg/m^3) (a) 420, (b) 397, and (c) 345 from a cross-section view (Continued).	68
4.18 d) Maximum stress (MPa) Time (s) plot for the model of filaments number 20 of and the density (kg/m^3) 420, 397, and 345.....	68

LIST OF FIGURES(Continued)

Figure	Page
4.19 Stress [MPa] in the gravity direction for the drop height 100 mm filaments number 15 and the density (kg/m^3) a) 420, and b) 397 from a cross-section view	69
4.20 Stress [MPa] in the gravity direction for the drop height 100 mm filaments number 15 and the density (kg/m^3) c) 345 from a cross-section view (Continued).	70
4.20 Stress [MPa] in the gravity direction for the drop height 100 mm filaments number 15 and the density (kg/m^3) c) 345 from a cross-section view (Continued).	70
4.21 Maximum stress (MPa) Time (s) plot for the model of filaments number 15 of and the density (kg/m^3) 420, 397, and 345.....	71
4.22 Maximum stress values for samples with filament numbers 15, 20, and 25, and densities of 420, 397, and 345 kg/m^3 drop test 100 mm was observed at 0.013 s after impact.	77

CHAPTER I

INTRODUCTION

1.1 Background and problem

Damage during transportation is a significant issue for fresh produce. Foam cushions are commonly used in the transport process, but these cushions are made from non-biodegradable materials, which creates a major waste problem. As an alternative, natural rubber latex (NR) is considered a suitable material choice, as NR is biodegradable. However, the manufacturing process of NR cushions involves numerous factors that must be addressed. To aid in solving this engineering problem, computer-aided design (CAD) software is used for the modification, analysis, and optimization of designs. CAD tools help improve the performance of models and create a database for manufacturing. In this study, the primary objective for the cushion design was to minimize physical damage. A 3D model of the cushion was created using SolidWorks software and simulated in ANSYS Workbench.

1.2 Research objectives.

1.2.1 To optimize the structural design parameters of natural rubber latex foam (NRLF) cushioning material for packaging applications.

1) To investigate the effects of filament number and filament diameter on the mechanical properties and cushioning performance of NRLF.

2) To study the influence of foam density variation on the impact of absorption efficiency and foam structure integrity.

1.2.2 To evaluate the impact protection performance of NRLF cushions using Finite Element Method (FEM) simulation.

- 1) To develop accurate CAD models of NRLF cushions and model fruit (Glom Sali guava) for drop test simulation.
- 2) To compare cushioning effectiveness of NRLF foam against commercial expanded polyethylene (EPE) foam and unprotected guava under various impact conditions.

1.2.3 To analyze the relationship between cushioning design parameters and maximum stress in fresh produce during impact.

- 1) To determine how variations in filament number, filament diameter, and foam density influence stress distribution and peak stress during simulated drop tests.
- 2) To identify optimal combinations of design parameters that minimize mechanical damage to fruit while maintaining lightweight and eco-friendly packaging solutions.

1.2.4 To demonstrate the feasibility of using computer-aided design (CAD) and FEM simulation as efficient tools for developing sustainable cushioning packaging.

- 1) To validate the FEM simulation approach as a time- and cost-effective alternative to traditional experimental testing.
- 2) To provide design guidelines for producing high-performance, environmentally friendly cushioning materials based on simulation results.

1.3 Goals

The goals are as follows.

- 1.3.1 Analyze and define the cushion performance of alternative materials.
- 1.3.2 Analyze and define damage of the foam net cushion design.
- 1.3.3 Analyze and define the foam net cushion design.

1.4 Scope and limitations

This study focuses on the development and evaluation of eco-friendly cushioning foam made from natural rubber latex foam (NRLF) for fruit packaging applications, with particular emphasis on impact protection performance. The research is divided into three main sections: first, the study compares the impact protection of unprotected guavas (without packaging) to those cushioned with commercial expanded polyethylene (EPE) foam through drop tests simulated at a height of 200 mm to evaluate cushion effectiveness under realistic impact conditions. Second, it investigates the effect of filament number (25, 20, and 15 filaments) and filament diameter (2.5, 3.5, and 4.5 mm) on the mechanical behavior and cushioning efficiency of NRLF cushions, with drop tests also conducted at 200 mm to assess cushioning under standard impact conditions. Third, the study explores how reducing foam density (420, 397, and 345 kg/m³) influences the cushioning performance of NRLF cushions with different filament numbers, where drop tests were simulated at a height of 100 mm to specifically evaluate the effect of density reduction on cushioning efficiency. NRLF cushions were modeled using CAD software (SolidWorks®) and simulated under explicit dynamic conditions in ANSYS® to replicate these drop tests, with the guava fruit represented as a homogeneous elastic body. The primary evaluation metric was the maximum stress experienced by the fruit during impact, which was used to infer cushioning performance.

1.4.1. Limitations of the study

- 1) The simulation assumes idealized material properties and uniform foam structures, which may differ from actual heterogeneous foam behavior and manufacturing variability.
- 2) The guava model does not account for internal biological complexity or anisotropic properties, potentially affecting the accuracy of stress predictions.

- 3) Environmental factors such as temperature, humidity, and long-term foam durability under real transportation conditions were not considered.
- 4) Experimental validation was limited to simulation results; physical drop tests and empirical data collection were outside the scope of this research.
- 5) The biodegradability and life cycle assessment of NRLF materials were not addressed in this study and remain areas for future investigation.

Despite these limitations, the findings provide useful insights into the design of sustainable cushioning foam and demonstrate the effectiveness of FEM simulations as a tool for packaging development.

1.5 Research benefits

This research provides several important benefits to the field of sustainable packaging and material engineering:

- 1) Development of Eco-Friendly Packaging Solutions: By focusing on natural rubber latex foam (NRLF) as a biodegradable and renewable cushioning material, the study contributes to reducing environmental impact compared to conventional synthetic foams like expanded polyethylene (EPE).
- 2) Optimization of cushion Design on cushion performance: The investigation into the effects of filament number, filament diameter, and foam density on cushioning performance offers valuable insights for designing lightweight yet effective protective packaging. This optimization can help reduce material usage and packaging weight, leading to cost savings and improved transport efficiency.
- 3) Advancement of simulation techniques: Employing Finite Element Method (FEM) simulations to evaluate cushioning performance allows accurate

prediction of mechanical behavior without extensive physical prototyping. This accelerates the development process and reduces experimental costs.

- 4) Enhanced fruit protection: The research improves understanding of how cushioning parameters influence impact protection, helping to minimize mechanical damage to sensitive fruits like guava during handling and transportation, thereby reducing food waste.

The proposed method was able to determine the damage for transport process from transport process. The damage problem mitigation with cushion packaging method in case of different cushion foam material is also investigated.



CHAPTER II

LITERATURE REVIEW

2.1 Introduction

This chapter provides a comprehensive review of foundational studies related to the finite element method (FEM), including simplified models frequently employed in drop impact analysis, material characterization, and nonlinear cushion modeling. In addition, various computational approaches utilized in the simulation of foam net cushioning systems are discussed.

2.2 Transportation damage

Mechanical damage is a critical factor influencing the postharvest quality of fruits during transportation. External forces such as impacts and vibrations are primary contributors to this form of deterioration. Specifically for guava, quality degradation during transit not only results in substantial economic losses but also exacerbates postharvest fruit waste.

Bruising refers to a form of latent mechanical injury that is not immediately visible upon occurrence (Mei et al. 2023). Such damage commonly arises during transportation, sorting, and packaging operations, and contributes significantly to the deterioration of kiwifruit. Due to its high susceptibility to mechanical stress, particularly from external impacts, kiwifruit is especially prone to this type of damage.

The primary cause of bruise damage during fruit handling is the application of excessive impact forces resulting from dropping onto packaging surfaces (Lin et al. 2023).

Similarly, reported that apples dropped onto rigid surfaces such as concrete or wood exhibited the most severe bruising (Stopa et al. 2018)., whereas foam surfaces

resulted in the least damage among four tested packaging materials during free-drop trials. Moreover, wooden packaging was found to provide inferior protection against mechanical injury when compared with telescopic fiberboard trays and plastic containers (Batt et al. 2019). Nonetheless, the extent of bruise damage in kiwifruit caused by impact with different packaging materials such as wood, high-density polyethylene (HDPE), and expanded polystyrene (EPS) remains inadequately understood.

2.3 Impact damage

Impact damage occurs when an object collides with a surface with sufficient force to rupture or separate cellular structures. The external manifestations typically include bruising or cracking. Common impact damage scenarios primarily arise from two mechanisms: the free fall of fruits from trees to the ground during harvesting operations, and dynamic impacts occurring between individual fruits or between fruits and packaging materials or containers. The latter damage mechanism results from various vibrational sources, including transportation vehicle vibrations, fruit containers subjected to transport-induced oscillations, and vibrations from conveyor belts in grading systems. Impact damage represents the most severe mechanical damage mechanism in fruit handling processes, significantly affecting post-harvest quality and economic value (Van Zeebroeck et al. 2007).

2.4 Impact damage to fresh produce

The two most common procedures for impact testing are: mounting the fruit with a pendulum impactor or dropping the fruit from a predetermined height onto an impact surface. In the drop test method, the impact energy (E_{impact}) is calculated using the equation $E = mgh$ where m is the mass of the sample (kg), g is the acceleration due to gravity (9.81 m/s^2), and h is the drop height (m).

2.4.1. Package cushioning

One of the fundamental objectives of packaging engineering is to ensure that a product is transported from the point of manufacture to the point of sale without sustaining unacceptable levels of damage or loss (Yam. 2010). Packaging particularly through the use of cushioning materials plays a vital role in mitigating in-transit damage. However, packaging solutions must not only be effective but also economically and practically feasible.(Al-Dairi et al. 2022).

Most products require protective packaging because they are typically engineered to endure only their intended usage conditions, rather than the rigorous and unpredictable stresses encountered during distribution (Goodwin et al. 2011). Among the various hazards present in the distribution environment, the most prevalent include impacts, punctures, and deformation from manual handling; vibrations induced by vehicle motion; compression resulting from stacking; atmospheric changes at high altitudes; and fluctuations in relative humidity and temperature (Hatton. 1998).

2.4.2. Packaging as a green solution.

In general, foam net cushion packaging used for fresh produce particularly vegetables and fruits is predominantly designed for single-use applications. These cushions are typically manufactured from synthetic, non-biodegradable polymers, which contribute significantly to post-consumer environmental waste. Concurrently, plastic waste pollution has emerged as one of the most critical global environmental concerns.

Within this context, biodegradable plastics represent both considerable challenges and compelling opportunities. These include the need to enhance material performance, ensure cost-effectiveness, and develop scalable manufacturing processes. At the same time, such materials offer the potential to substantially mitigate the long-term environmental impacts associated with conventional plastic waste.

2.5 Finite element method

Principles finite element method The FEM process begins with discretizing the domain of the problem into smaller, simpler parts called elements. These elements are then analyzed using numerical techniques (Figure 2.1), often derived from partial differential equations, to obtain an approximate solution across the entire domain.

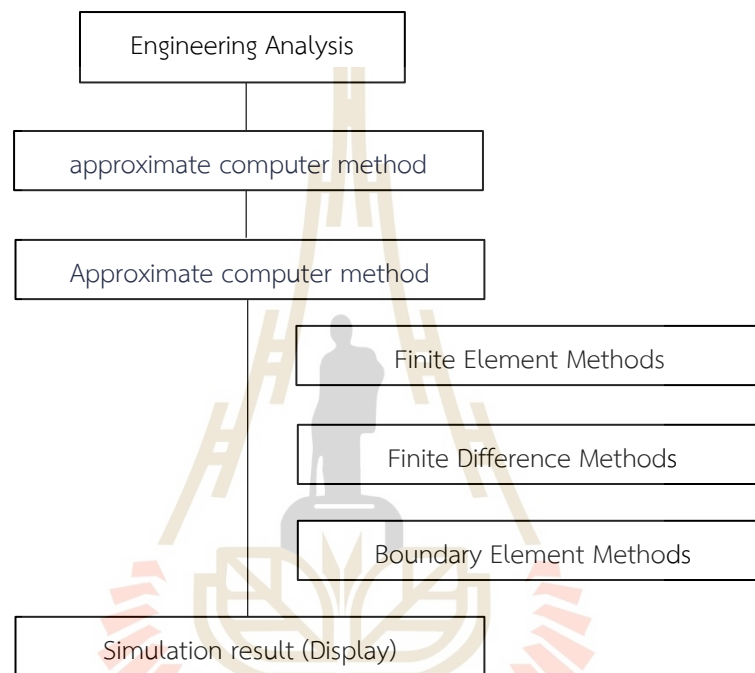


Figure 2.1 The process of computer aid designs and numerical techniques

The Finite Element Method (FEM), also known as Finite Element Analysis (FEA), is a computational technique used to obtain approximate solutions to boundary value problems in engineering. FEM is a numerical method that provides approximate solutions for a wide range of complex engineering problems. It has become an essential tool in modern engineering as shown in (Figure 2.2), extensively applied in the analysis, simulation, and design of real-world systems.

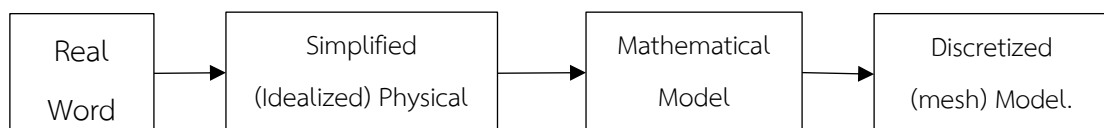


Figure 2.2 Workflow of pre-processing FEM simulation

2.5.1. Differential equation

Differential equation is partial differential (PDE), ordinary differential equation (ODE) is a equation that involves two or more unknown functions. Such equations aid in the relationship of function with several variables to their partial derivatives.

General Form of first-order partial derivatives equation.

A first-order partial derivative equation with n independent variables has general form.

$$F(x_1, x_2, \dots, x_n, w, \frac{\partial w}{\partial x_1}, \frac{\partial w}{\partial x_2}, \dots, \frac{\partial w}{\partial x_n}) = 0, \quad (1)$$

Where: $w=w(x_1, x_2, \dots, x_n)$ is the unknown function

$F(\dots)$ is a given function.

Order of partial differential equations

$$\frac{\partial z}{\partial x} + \frac{\partial z}{\partial y} = x + zy \quad (2)$$

As the order of the highest derivative is 1.

Degree of partial differential equations

$$\frac{\partial z}{\partial x} + \frac{\partial z}{\partial y} = z + xy \quad (3)$$

Has 1 as the highest derivative is of the first degree.

2.6 FEM for solid mechanics problems

Equilibrium of rigid body and elastic behavior of solids

Triaxial stress represents a stress state wherein a stress element is subjected to three mutually perpendicular normal stresses, shown in (Figure 2.3). The absence of shear stresses on the x , y , and z planes indicates that these three normal stresses constitute

the principal stresses of the system. This configuration is fundamental to the analysis of material behavior under complex loading conditions.(Gere et al. 1997).

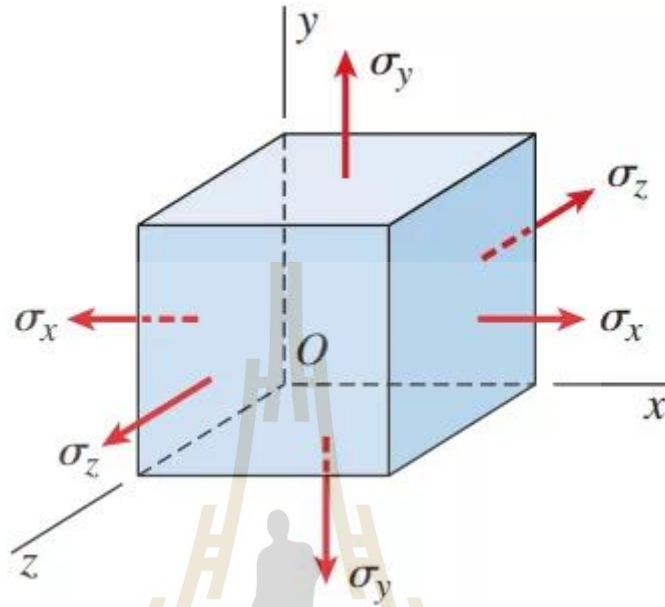


Figure 2.3 Triaxial Stress State (James Gere, 2008.)

Rigid objects in static equilibrium equation

$$\frac{\partial \sigma_x}{\partial x} + \frac{\partial \tau_{xy}}{\partial y} + \frac{\partial \tau_{xz}}{\partial z} + F_x = 0 \quad (4)$$

$$\frac{\partial \tau_{xy}}{\partial x} + \frac{\partial \sigma_y}{\partial y} + \frac{\partial \tau_{yz}}{\partial z} + F_y = 0 \quad (5)$$

$$\frac{\partial \tau_{xz}}{\partial x} + \frac{\partial \tau_{yz}}{\partial y} + \frac{\partial \sigma_z}{\partial z} + F_z = 0 \quad (6)$$

Where: $\sigma_x, \sigma_y, \sigma_z$ is axial or longitudinal stress x, y, z.

$\tau_{xy}, \tau_{xz}, \tau_{yz}$ is shear stress in axial x, y, z.

F_x, F_y, F_z is body force in axial x, y, z.

2.6.1. Surface traction

Boundary conditions may consist of many systems. One of the conditions is surface traction in general.

2.6.1.1 Traction (Stress) Vector

The traction vector (T) is defined as the ratio of the force vector acting upon a specified cross-section to the area of that cross-section. This fundamental parameter characterizes the distributed force intensity across the material interface and serves as a critical measure in continuum mechanics analyses

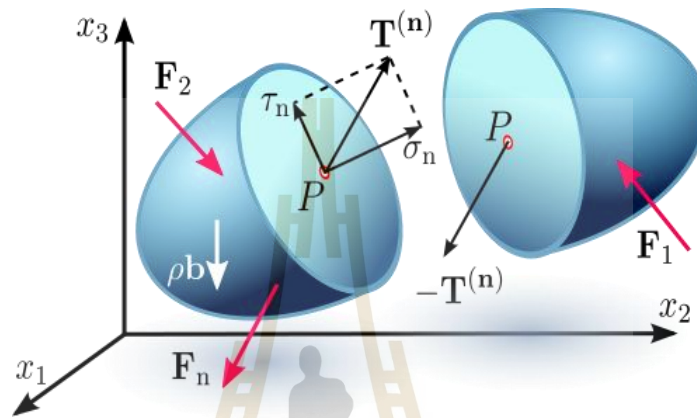


Figure 2.4 The traction vector (T), (stress vector at the point) on the surface surrounding the point with normal vector \mathbf{n} is defined as.

Figure 2.4 depicts the stress vector T acting on an internal surface within a continuum, illustrating both normal and shear stress components on this surface. Additionally, the figure demonstrates the reaction stress vector $-T$ operating on the opposing side of the internal surface, in accordance with Newton's Third Law of Motion, which stipulates the equivalence of action and reaction forces. This representation elucidates the fundamental stress transmission mechanism across internal material boundaries and the inherent equilibrium properties of continuous media under mechanical loading conditions (Truesdell. 1976).

$$T_n = \lim_{\Delta A \rightarrow 0} \frac{\Delta F}{\Delta A} \quad (7)$$

from Newton's laws of motion: $T_n = -t_{-n}$

$$T = \frac{F_{internal}}{Area} \quad (8)$$

Stress Tensors and Traction Vectors.

$$\vec{T} = T_x \hat{i} + T_y \hat{j} + T_z \hat{k} \quad (9)$$

Where: T_x, T_y, T_z is stress at surface in axial x, y, z respectively

$$\begin{Bmatrix} T_x \\ T_y \\ T_z \end{Bmatrix} = \begin{Bmatrix} \sigma_x & \tau_{xy} & \tau_{xz} \\ \tau_{xy} & \sigma_y & \tau_{yz} \\ \tau_{xz} & \tau_{yz} & \sigma_z \end{Bmatrix} \begin{Bmatrix} n_x \\ n_y \\ n_z \end{Bmatrix} \quad (10)$$

Where: n_x, n_y, n_z is vector cosine direction

$$n = n_x \hat{i} + n_y \hat{j} + n_z \hat{k} \quad (11)$$

Boundenly condition vector vertical of surface the rigid body possible body possible show pre-strain shows the relationship between normal strain and normal stress. As shown in Figure 2.5

$$\{\sigma\} = [c]\{\epsilon - \epsilon_0\} \quad (12)$$

For

$$\{\sigma\}^T = [\sigma_x \ \sigma_y \ \sigma_z \ \tau_{xy} \ \tau_{yz} \ \tau_{xz}] \quad (13)$$

$$\{\epsilon\}^T = [\epsilon_x \ \epsilon_y \ \epsilon_z \ \gamma_{xy} \ \gamma_{yz} \ \gamma_{xz}] \quad (14)$$

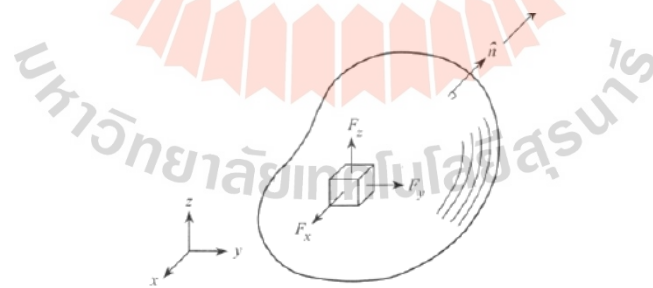


Figure 2.5 Rigid body equilibrium 3D

$$[C] = \frac{E}{(1+\nu)(1-2\nu)} \begin{bmatrix} 1-\nu & \nu & \nu & 0 & 0 & 0 \\ \nu & 1-\nu & \nu & 0 & 0 & 0 \\ \nu & \nu & 1-\nu & 0 & 0 & 0 \\ 0 & 0 & 0 & \frac{(1-2\nu)}{2} & 0 & 0 \\ 0 & 0 & 0 & 0 & \frac{(1-2\nu)}{2} & 0 \\ 0 & 0 & 0 & 0 & 0 & \frac{(1-2\nu)}{2} \end{bmatrix} \quad (15)$$

Where: ν is Poisson's ratio

Matrix $[C]$ show the relationship between stress and strain and $\{\epsilon_0\}$ are pre strain.

And

$$\{\epsilon_0\}^T = [\Delta T \ \Delta T \ \Delta T \ 0 \ 0 \ 0] \quad (16)$$

2.6.2. Three-dimensional isoperimetric elements.

Calculation of strains and stresses

Strains inside an element are determined with the use of the displacement differentiation matrix.

$$\{\epsilon\} = [B] \quad (17)$$

Stresses are calculated with the Hook's law.

$$\{\epsilon\} = [E]\{e\} = [E](\{\epsilon\} - \{\epsilon_0\}^T) \quad (18)$$

Where $\{\epsilon_0\}^T$ is the vector of free thermal expansion.

2.7 Mesh generation

The successful of the finite element method simulation is the mesh generation show in Figure 2.6 (Sadrehaghighi. 2021)., In general hexahedral element was general element as it shows great accuracy and flexibility, in engineering problem CAD simulation very complex geometries hexahedral element impossible to generating, the complex

geometries trihedral element was flexibility and great the generating process show in Figure 2.7

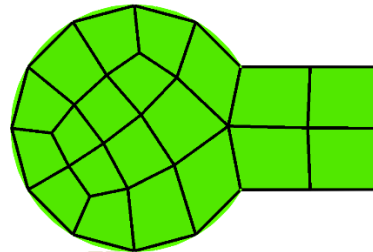


Figure 2.6 Finite element mesh of quadrilaterals of a curved domain.

Mesh generation process

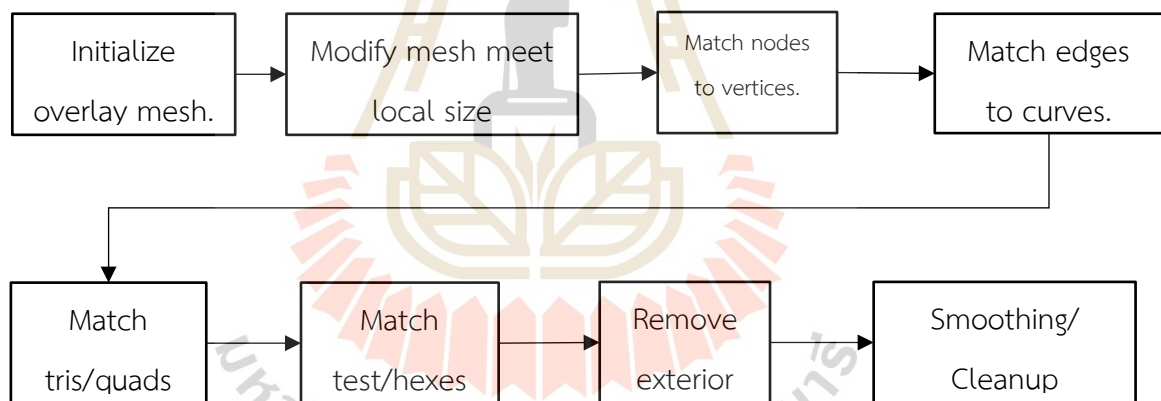


Figure 2.7 Mesh generation

2.8 Failure theories of material

The finite element method analysis to solve an engineering problem is defined by testing method by Yield Strength (σ_y) or Ultimate Strength (σ_u) are Failure analysis. The Failure analysis of martial consists of two types: Ductile Materia and Brittle Material, stress-strain curves as shown in Figure 2.8

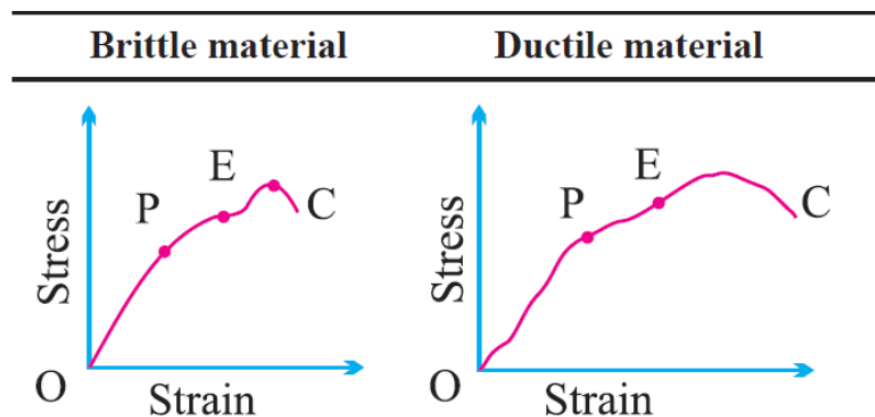


Figure 2.8 Stress-strain curves of brittle material, ductile material-compression test

2.8.1. Brittle fracture

For a brittle material, brittle fracture takes place without any appreciable deformation, and by rapid crack propagation. The direction of crack motion is very nearly perpendicular to the applied tensile stress and yields a relatively fractured surface.

2.8.2. Ductile fracture

When ductile material has a gradually increasing tensile stress, it behaves elastically up to a limiting stress and then plastic deformation occurs. As stress is increased, the cross-sectional area of the material is reduced, and a necked region is produced.

A comprehensive universal theory of failure that encompasses all material properties and stress states remains elusive in continuum mechanics. Rather, the field has evolved through multiple hypotheses formulated and experimentally validated over several decades, as shown in Figure 2.9. This evolutionary process has culminated in a collection of contemporary methodologies widely adopted by engineering practitioners. These methodologies, while not universally applicable across all material systems, provide pragmatic frameworks that guide modern design practices and failure prediction protocols in various engineering disciplines.

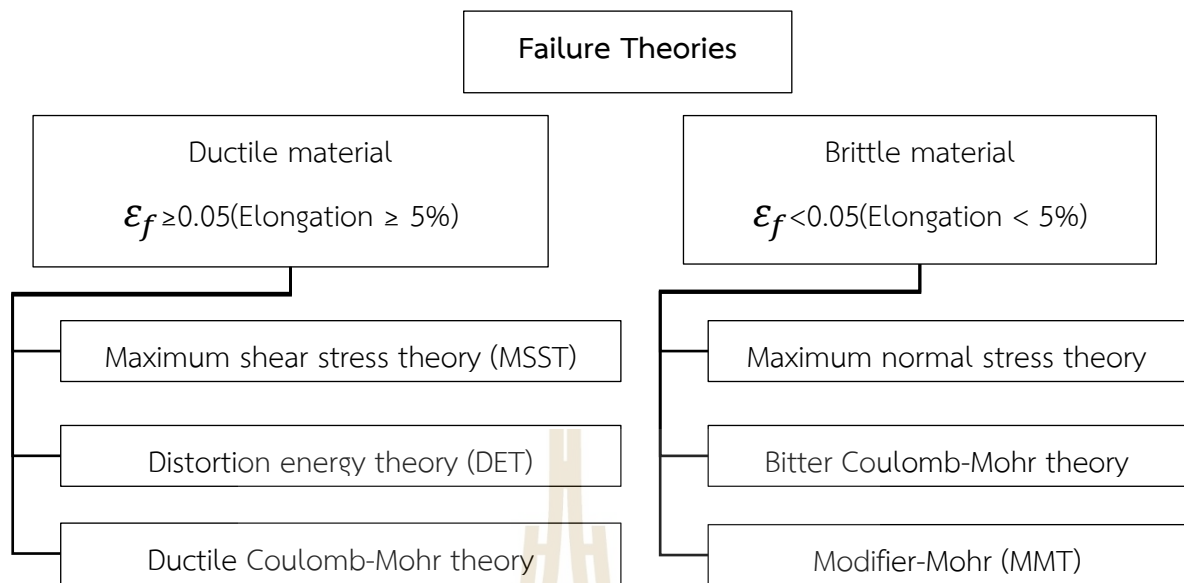


Figure 2.9 Diagram failure theories of material

Historical development of failure theories showing the relationship between theoretical models and their experimental validation. The convergence towards contemporary design methodologies is highlighted, demonstrating the progressive refinement of failure prediction capabilities over time.

2.8.3. Triaxial stress

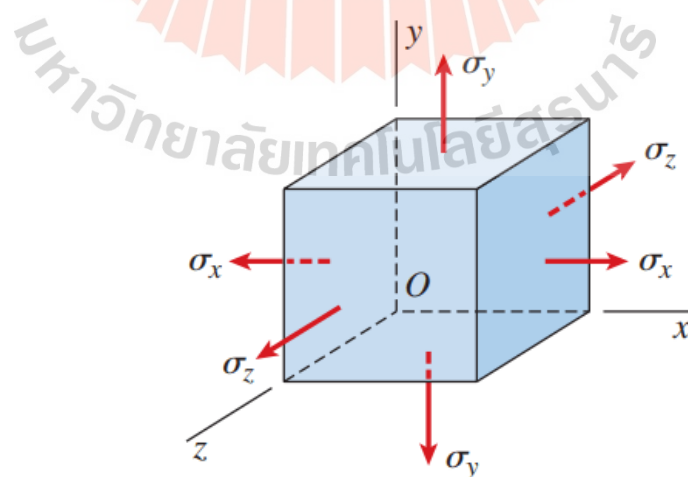


Figure 2.10 Triaxial stress state mechanics of materials (James Gere, 2008)

Triaxial stress is the stress state when a stress element is acted upon by three mutually normal stresses on the x, y, and z planes so the three normal stresses are the principal stresses.

Yield Strength (σ_y) ductile materials

Ultimate Strength (σ_u) brittle materials

Failure theories are defined as a function of the principal stress and the materials.

$$f(\sigma_1, \sigma_2, \sigma_3) = \sigma_x, \sigma_y \quad (19)$$

Probably the simplest failure theory is to the failure occurred when the maximum or minimum principal stress as reach the yield or ultimate strengths of the material.

Rankine (maximum principal stress)

$$\sigma_1 = \sigma_y, \sigma_u \quad (20)$$

$$\sigma_3 = -\sigma_y, -\sigma_u \quad (21)$$

Maximum principal stress theory or Rankin theory

Failure of ductile materials

Hydrostatic stress does not cause yielding in ductile materials.

A general triaxial stress state like the one show decomposed into stresses which cause a change in volume and stress which cause shape distortion. Maximum Shear Stress

Elastic material show failure when Maximum Shear Stress higher than uniaxial stress tests show in Figure 2.11

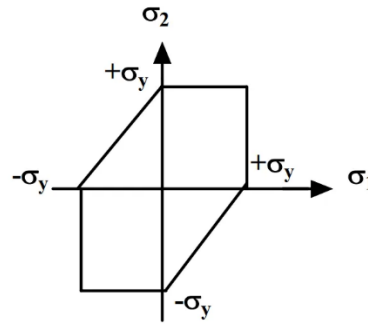


Figure 2.11 failure envelope as per maximum shear stress theory

$$\sigma_{eff} = \tau_{max} = \frac{\sigma_1 - \sigma_3}{2} \geq \frac{s_y}{2} \quad (22)$$

Where: $\sigma_A \geq \sigma_B \geq \sigma_C$ and $\sigma_A \geq \sigma_B$

- 1.) $\sigma_A \geq \sigma_B \geq 0$ by $\sigma_1 \geq \sigma_A$ and $\sigma_3 = 0, \sigma_A \geq s_y$
- 2.) $\sigma_A \geq 0 \geq \sigma_B$ by $\sigma_1 \geq \sigma_A$ and $\sigma_3 = 0, \sigma_A - \sigma_B \geq s_y$
- 3.) $0 \geq \sigma_A \geq \sigma_B$ by $\sigma_1 \geq \sigma_A$ and $\sigma_3 = \sigma_B \geq s_y$

Maximum Shear Stress theory creep failure

2.8.4. Von-Mises yield criteria.

The von Mises stress criterion serves as a principal methodology for predicting yield initiation in isotropic, ductile metallic materials subjected to complex loading conditions (Figure 2.12). This approach involves calculating the scalar von Mises stress value and comparing it with the material's yield stress, thereby implementing the von Mises Yield Criterion. The fundamental objective of this criterion is to establish a universally applicable yield prediction framework for ductile metals under arbitrary three-dimensional stress states, irrespective of the specific combination of normal and shear stresses present in the system. The von Mises stress effectively distills a complex triaxial stress state into a single scalar parameter that can be directly compared to the material's yield strength—a scalar value typically determined through uniaxial tensile testing, which represents the most straightforward experimental methodology for material characterization.

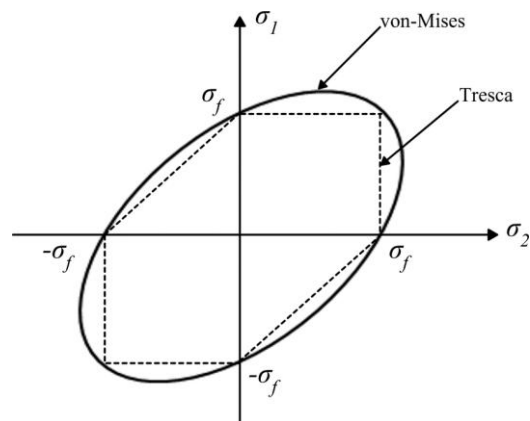


Figure 2.12 Comparison of the yield locus for the plane stress of von Mises yield criterion and Tresca yield criterion.

Figure 2.12 Three-dimensional representation of the von Mises yield surface in principal stress space. The cylindrical yield surface demonstrates the independence of yielding from hydrostatic stress components. The circular cross-section perpendicular to the hydrostatic axis ($\sigma_1 = \sigma_2 = \sigma_3$) distinguishes the von Mises criterion from other yield criteria such as Tresca (hexagonal).

CHAPTER III

METHODOLOGY

3.1 Material

3.1.1 NRL Foam

Natural rubber latex foam (NRLF) is a porous material exhibiting excellent mechanical properties, produced by foaming natural rubber latex followed by curing. NRLF has found widespread application in packaging materials. (Eaves. 2004). NRLF is synthesized using the Dunlop show in Figure 3.1, which involves whipping the latex into a froth, molding, and vulcanizing to achieve the desired foam structure (Blackley. 1997).

Table 3.1 Formulation of the natural rubber latex (NRL) compounds for the synthesis of reinforcing NRL foam (NRLF).

Ingredients	Content (phr ¹)	Functions
60% High ammonia natural rubber latex (HA Latex)	100.00	Matrix
10% Potassium oleate (K-oleate)	4.50	Foaming agent
50% Sulfur	2.00	Vulcanizing agent
50% Zinc diethylthiocarbonate (ZDEC)	2.00	1st accelerator
50% Zinc 2-mercaptobenzothiazone (ZDMT)	2.00	2nd accelerator
50% Wingstay L	2.00	Antioxidant
50% Zinc oxide (ZnO)	5.00	Activator
12.5% Sodium silicofluoride (SSF)	1.00	1st gelling agent
33% Diphenyl guanidine (DPG)	1.40	2nd gelling agent

¹Parts per hundred rubbers.

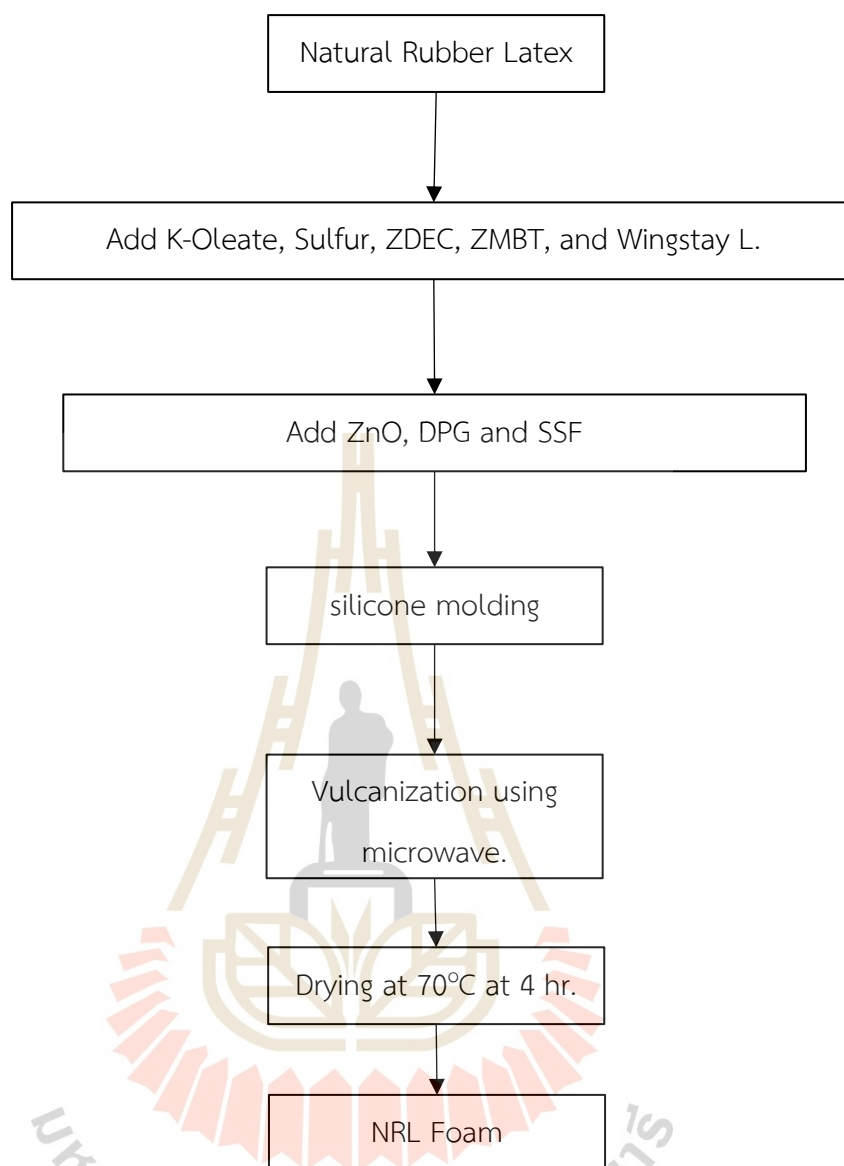


Figure 3.1 Flowchart of processing step NRL foam

3.1.2. Cushioning materials and testing

Mechanical properties were measured using a Universal Testing Machine (UTM) Instron Model 5560. A 1 kN load cell was employed, and the crosshead speed was set at 12 mm/min. Foam specimens, 3 mm thick, were cut into 100 mm × 100 mm square shapes. The compressive strength was reported at 50% strain. The cushion coefficient (C) serves as an indicator of cushioning performance, representing a material's ability to absorb energy under stress.(Xiao et al. 2022).The cushion coefficient was determined from the compressive stress-strain curve using the following equation:

Cushion coefficient. The cushion coefficient (C) is an ability of a cushion material to absorb the applied energy. The calculation was carried out using the data from the compression test mentioned earlier. The cushion coefficient equation is as follows

$$c = \frac{\sigma}{e} \times 100 \quad (23)$$

Where σ is the compressive stress (N/mm²), e is the energy absorption of the material (N·mm/mm³), which is estimated from the compressive stress–strain curve using

$$e = \int_0^e \sigma d\epsilon \quad (24)$$

Where ϵ is the compressive strain (mm/mm).

3.1.3. Testing Method

ASTM D3574 Standard Test Methods for Flexible Cellular Materials-Slab, Bonded, and Molded Urethane Foams

ASTM D3574 C is one such testing method that comprises a range of tests to specify the several properties of the foam. This consists of measurements of odor, dynamic force responses, foam density, aging, and mechanical properties.

The specified standard specimen for ASTM D3574 test C is recommended to have minimum dimensions of 50 mm in length, 50 mm in width, and 25 mm in

thickness as shown in Figure 3.2. While this represents the lower limit, it is advisable to utilize larger specimens. Ideally, the specimen's surface area should be a minimum of 2500 mm², coupled with a minimum thickness of 20 mm.



Figure 3.2 Sample cube specimen of 50 mm X 50 mm X 25 mm used in the study.

Achieving accuracy in finite element method simulations necessitates the precise definition of a material's mechanical properties

Material property using finite element methods included Modulus of elasticity, Yield stress, Poisson's ratio.

Mechanical properties were measured using a Universal Testing Machine (UTM) Instron Model 5560. The INSTRON Control module to develop systematic test methodologies for materials evaluation. The Control module enables the design of precise, multi-stage testing protocols with predefined displacement or force parameters, allowing for comprehensive material characterization under controlled conditions. The experimental apparatus utilized was the INSTRON/5565 universal testing machine, as shown in Figure 3.3, which provided the necessary mechanical precision and data acquisition capabilities required for this investigation.



Figure 3.3 Universal testing machine (INSTRON/5565, Norwood, MA, USA).

Investigation was performed on a rigid natural rubber latex foam material of density 272.06 kg/m^3 . The natural rubber latex foam specimens size used where dimension $50 \text{ mm} \times 50 \text{ mm} \times 25 \text{ mm}$ as shown in Figure 3.5

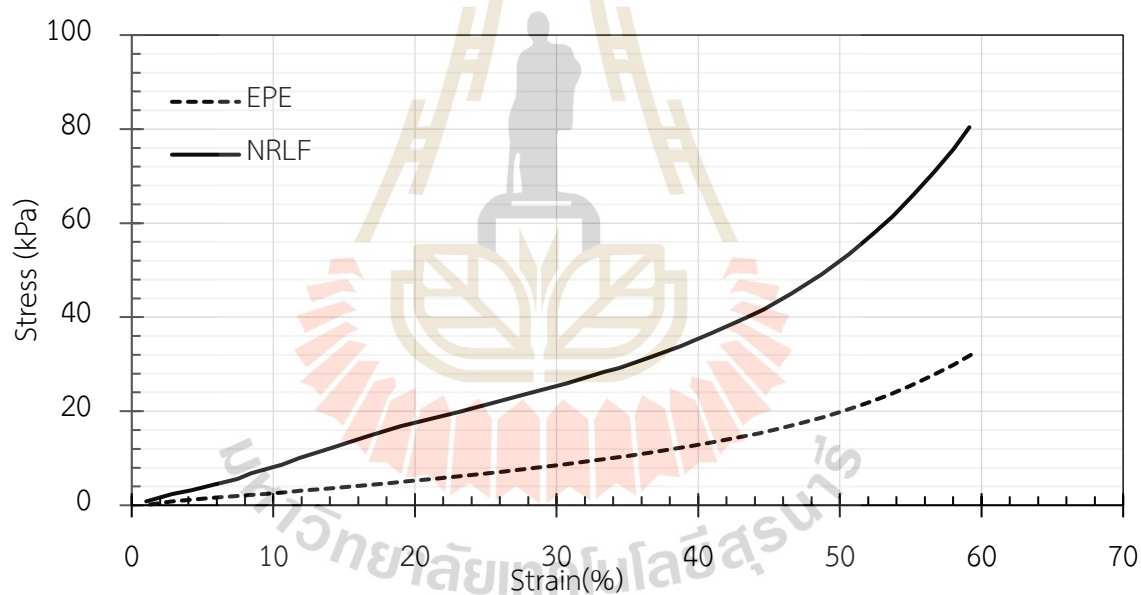


Figure 3.4 Stress-strain curve of the EPE and NRLF foam obtained using a compression test.

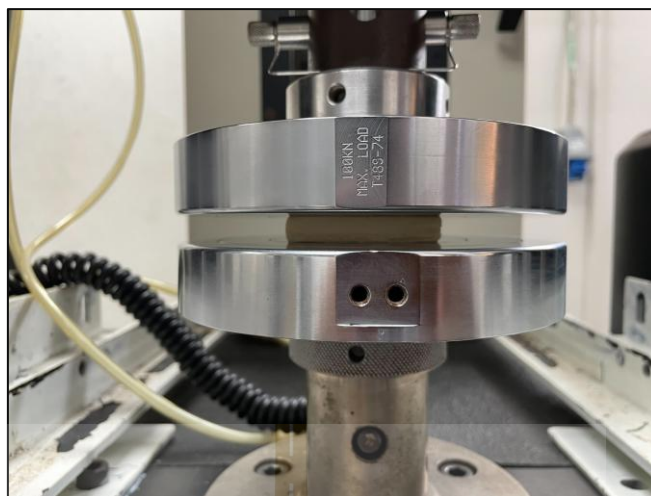


Figure 3.5 Sample cube specimen of 50 mm X 50 mm X 25 mm follower ASTM D3574 test C under compression testing.

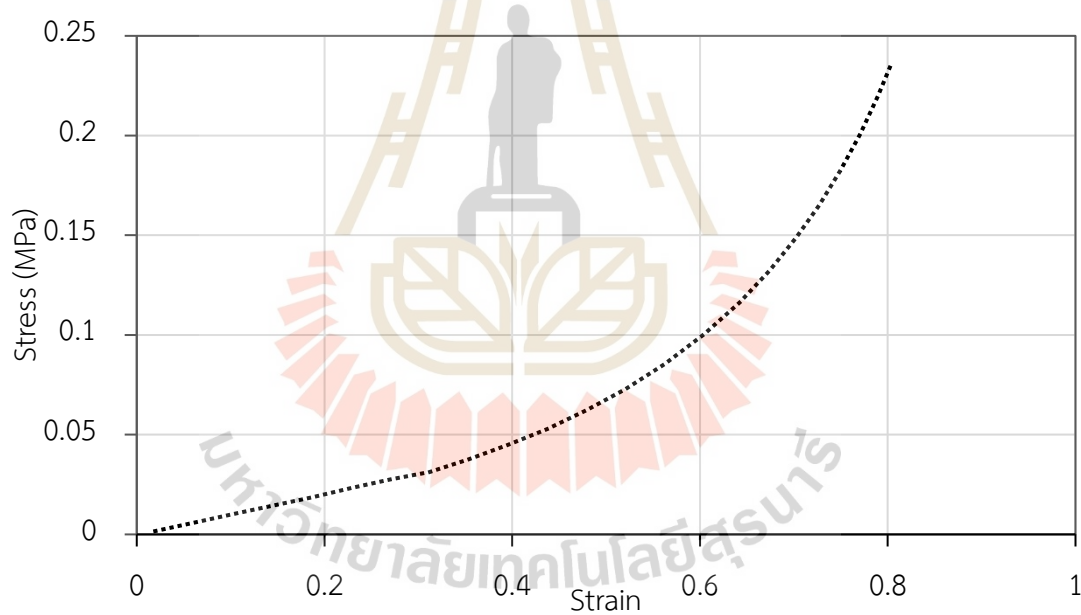


Figure 3.6 Stress-strain curve of the EPE foam obtained using a compression test.

Table 3.2 Compressive stress at 50% Strain of foam samples

Cushion foam	Compressive stress at 50% Strain (kPa)
EPE	18.75
NRLF	56.85

3.1.4. Mechanical Characterization of Guava Under Compression

Compressive testing is a fundamental mechanical characterization technique used to assess a material's ability to withstand loads that tend to reduce size. When applied to biological materials such as fruit, compressive testing provides insight into the deformation behavior, failure mechanisms, and structural integrity of the cellular matrix. In the case of guava, which has a heterogeneous internal structure comprised of soft parenchymatous tissue and denser seed cavities, the compressive response is expected to be non-linear and highly dependent on factors such as maturity, moisture content, loading rate, and orientation. The objective of this investigation is to systematically characterize the compressive behavior of guava under quasi-static loading conditions. Emphasis is placed on the influence of specimen orientation, size, and maturity on the resulting mechanical parameters.

3.1.5. Characterization of Mechanical Properties

Compressive testing represents a fundamental mechanical characterization method, widely employed to evaluate materials' resistance to externally applied loads that induce size reduction. In the context of biological materials, particularly fruits, compressive testing elucidates deformation behavior, failure mechanisms, and structural integrity of cellular matrices. Guava (*Psidium guajava* L.), known for its heterogeneous internal architecture comprising soft parenchymatous tissue surrounding comparatively denser seed cavities exhibit complex, non-linear compressive responses. This behavior is strongly influenced by factors such as fruit maturity, moisture content, loading orientation, and strain rate.

In this investigation, the compressive behavior of the 'Glom Sali' guava cultivar was systematically characterized under quasi-static loading conditions. Particular emphasis was placed on the influence of sample orientation, maturity level, and geometric parameters on the resulting mechanical responses. To support finite element modeling of guava deformation, both physical and mechanical properties were experimentally determined.

A total of ten mature guava fruits, each weighing between 250 and 300 grams, were randomly selected for preliminary characterization. The average density and volume were determined to be 1.24 ± 0.07 g/mL and 194.6 ± 17.73 mL, respectively. The measured average horizontal width and vertical length were 7.5 cm and 8.0 cm, respectively, with a mean fruit weight of 239.1 g. Additional mechanical parameters, such as firmness (4.68 N), were recorded to facilitate the estimation of material stiffness. Key physical attributes—including diameter, uniformity, and maturity were also documented, as these parameters directly influence mechanical response under compressive loading.

For compression testing, cubic specimens with dimensions of 20 mm x 20 mm were extracted from the equatorial region of the fruit (Figure 3.7).

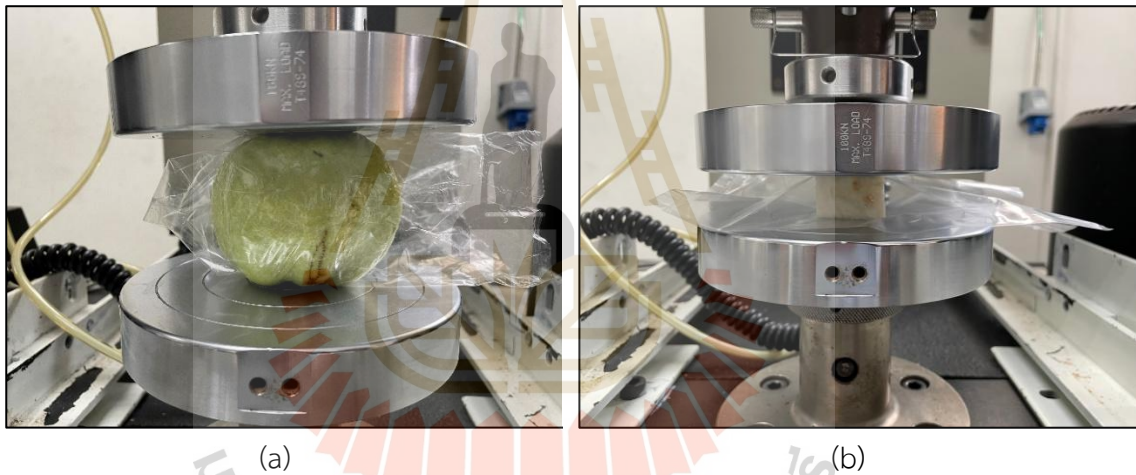


Figure 3.7 (a) Guava fruit (*Psidium guajava* L.) cv. Glom Sali (b) Sample cube specimen of guava (*Psidium guajava* L.) using in the present study sample size 20 mm x 20 mm.

Young's modulus (Y) was determined by measuring the equatorial diameter of the fruit (d) and subsequently substituting this value into the following equation.

$$Y = \frac{\sigma}{\varepsilon} \quad (25)$$

Where: $\sigma = \frac{4F}{\pi d^2}$, $\varepsilon = \frac{d_i - d_f}{d_i}$ the strain of the guava,

σ is a measure of the force acting on a unit area of a material

ϵ is the deformation of a material from stress

d_i is equatorial diameter of the deformed fruit

d_f is equatorial diameter of the intact fruit

Alternatively, the acoustic impact test can be utilized to determine Young's modulus by incorporating the values of fruit firmness (Sc) and density (ρ) into the following equation.

$$Y = Sc \rho^{1/3} \quad (26)$$

Where: Sc is the stiffness coefficient ($\text{Kg}^{2/3}/\text{s}^2$), f the dominant resonant frequency where the response magnitude is greatest (Hz) and m the fruit mass (g).

The Sc is significantly correlated with fruit firmness and sensory measurements (Galili and De Baerdemaeker 1996).

$$Sc = f^2 m^{2/3} \quad (27)$$

The stress-strain profile obtained from quasi-static compression tests (Figure 3.8) demonstrates the inherently non-linear response of guava tissue under load. The initial elastic regime is followed by a yielding region and subsequent densification, typical of porous, viscoelastic biological materials. These experimentally derived parameters are intended to inform and calibrate the finite element model simulating internal stress distribution and failure propagation within the guava matrix.

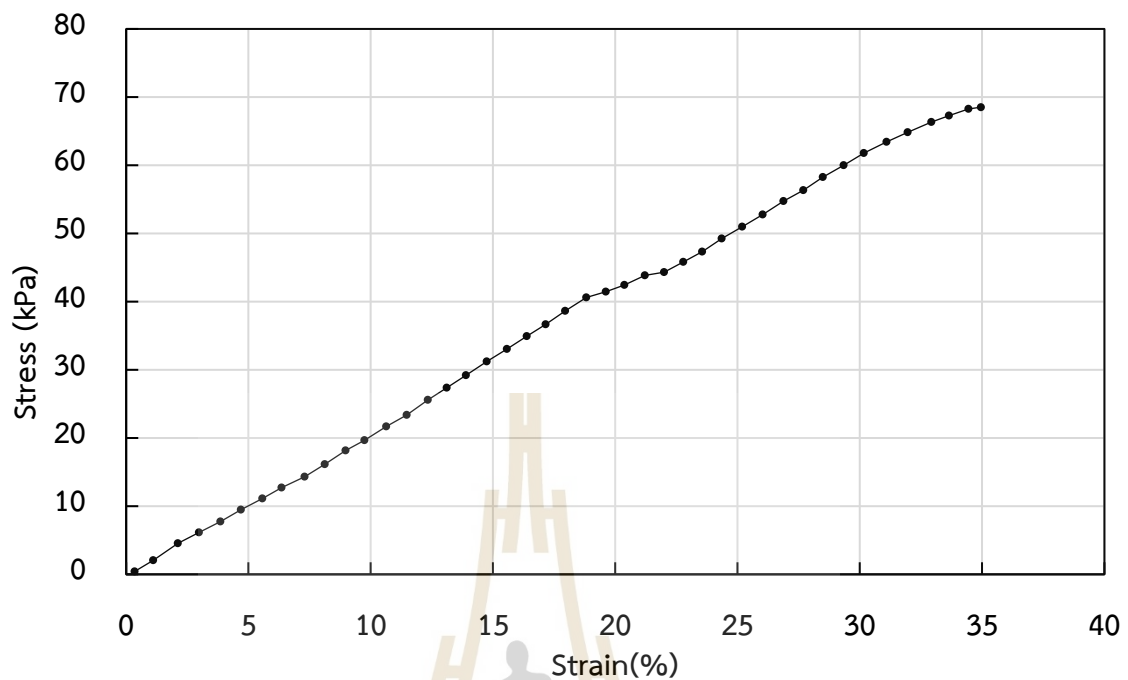


Figure 3.8 Stress-strain curve of the Guava (*Psidium guajava* L.) obtained using a compression test.

3.1.6. Poisson's ratio

Negative Poisson's ratio

The Poisson's ratio of a material describes the relationship between the transverse strain (expansion or contraction in the horizontal direction) and the axial strain (extension or compression in the vertical direction as shown in Figure 3.9).

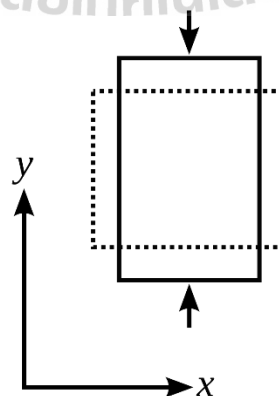


Figure 3.9 The Poisson's ratio of a material

The x-axis, with a Poisson's ratio of 0.5. The original green cube experiences no strain, while the red cube undergoes an expansion of ΔL in the x direction due to tension. Simultaneously, it contracts in the y and z directions by $\Delta L'$ as shown in Figure 3.10

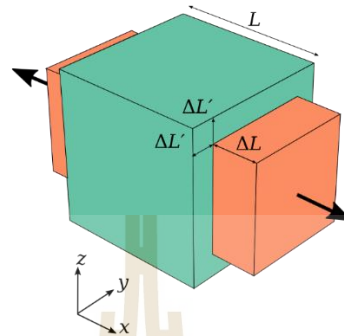


Figure 3.10 A cube made of an isotropic linearly elastic material is stretched along

Schematic explanation of the two-dimensional Poisson effect. **(A)** A two-dimensional depiction of an elastic material. **(B–D)** Schematic depictions about how the material **(A)** deforms under **(B)** horizontal stretching, **(C)** vertical squashing, and **(D)** vertical stretching from the top. Each depiction is accompanied by related horizontal and vertical deformation vectors shown in Figure 3.11 (Vijayakumar et al. 2021).

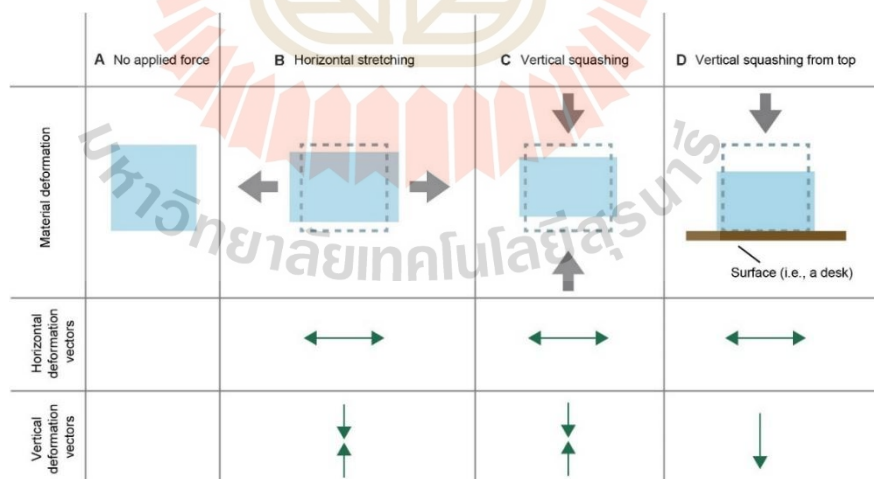


Figure 3.11 Schematic explanation of the two-dimensional poisson effect

Poisson's ratio of material

Samples used for Tests Guava consisted of dimensions of 15 mm × 15 mm with a thickness of 20 mm as shown in Figure 3.12. The compression speed 5 mm/min stop at 50% strain the as shown in Table 3.3.

$$\nu = \frac{-\varepsilon_x (\text{Lateral strain})}{\varepsilon_z (\text{Longitudinal strain})} \quad (28)$$

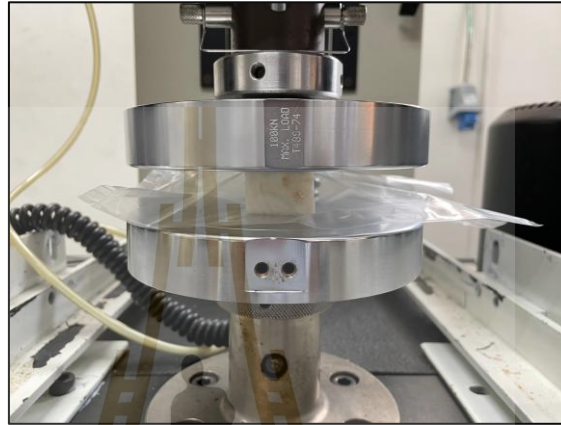


Figure 3.12 Sample cube specimen of guava (*Psidium guajava* L.) using in the present study sample size 20 mm x 20 mm.

Samples used for Tests NRLF consisted of dimensions of 20 mm × 20 mm with a thickness of 25 mm. Compression speed 50 mm/min stop at 50% strain the force displacement curve show in Figure 3.13.



Figure 3.13 Determine of NRLF negative Poisson's ratio using UTM.

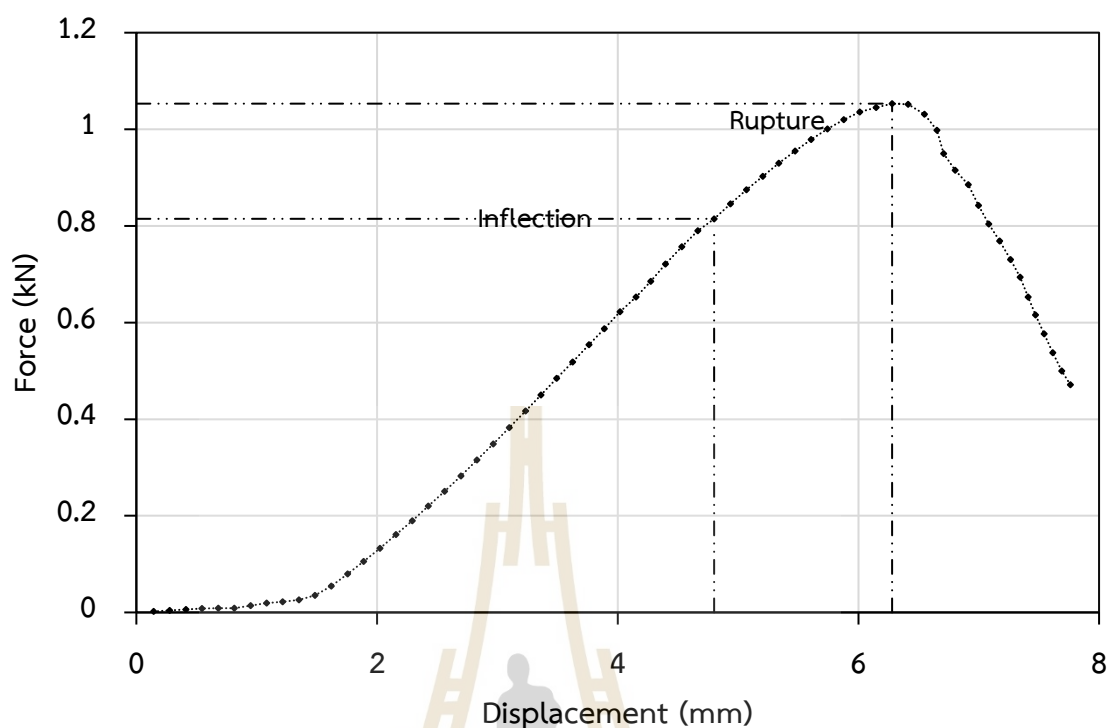


Figure 3.14 Force displacement curve of Guava fruit (*Psidium guajava* L.) Glom Sali

Table 3.3 Mechanical properties of foam samples and guava

Sample	Density ρ (Kg/m ³)	Compress stress at $\epsilon_{50\%}$ (kPa)	Young's modulus Y , (KPa)	Poisson's ratio ν
EPE	118±1.810	20.13±2.130	39.977	0.330±0.105
NRLF	272.06±3.450	56.85±3.560	105.482	0.337 ± 0.153
Guava	1240±0.070	53.53±28.320	20.739±10.242	0.490 ± 0.023

3.2 Computer-aided design

This section presents the problem simulation of drop test of guava with cushion net foam using ANSYS simulation and modeling 3D-model using Solid Work software.

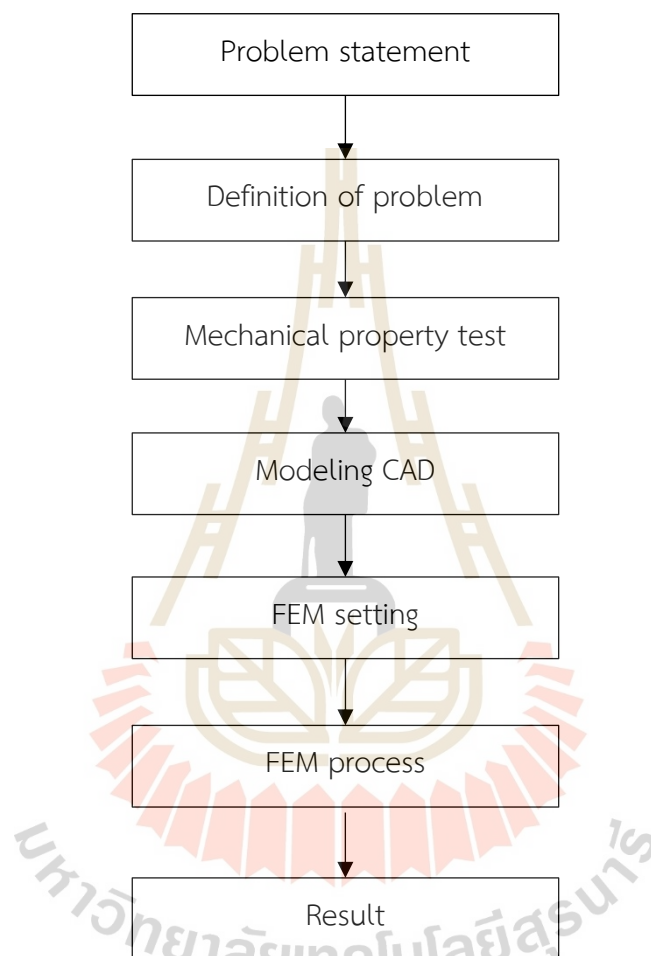


Figure 3.15 Flow chart of CAD/CAE design analysis (Chang. 2013).

3.3 Finite element analysis

3.3.1. Model Analysis

In the development of a reliable finite element model for evaluating fruit cushioning systems, the accuracy of the geometric representation is of paramount importance. This chapter presents the CAD modeling procedure for the guava fruit covered with a commercial expanded polyethylene (EPE) Figure 3.16 foam net, alongside

the design of an alternative natural rubber latex foam (NRLF) net structure. Given the complex nature of foam materials, appropriate simplifications were introduced to balance model fidelity with computational efficiency. Key geometric parameters were obtained from direct measurements and product specifications to ensure that the models accurately reflect the physical configurations used in real-world applications. The resulting CAD models serve as the foundational inputs for subsequent finite element analyses focused on impact performance



Figure 3.16 Guava with commercial expanded polyethylene foam net CAD Modeling
NRLF net foam cushion

3.3.2. Preprocess

The CAD modeling process began with the digital reconstruction of the guava's external geometry. A simplified spherical approximation was adopted to represent the guava, based on an average diameter measured from sampled fruits. The foam net was subsequently modeled by wrapping the guava with a network of interconnected struts, forming a lattice-like protective layer. For the commercial EPE foam net, standard cell shapes and connection patterns were replicated using a periodic unit cell approach. The alternative NRLF net was similarly designed but with adjusted cell dimensions and strut thicknesses to reflect the mechanical properties of the proposed material. The entire modeling process was conducted using SolidWorks® 2024, with attention to ensuring compatibility with finite element preprocessing software.

3.3.2.1 Geometry

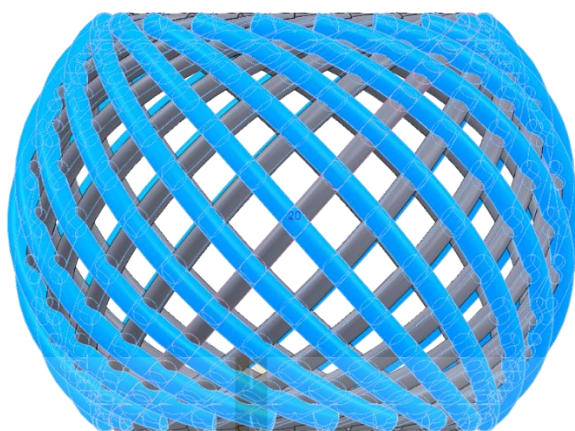


Figure 3.17 CAD cushion foam net 20 mesh filament number on NRLF 3.5 mm

3.3.2.2 CAD modeling

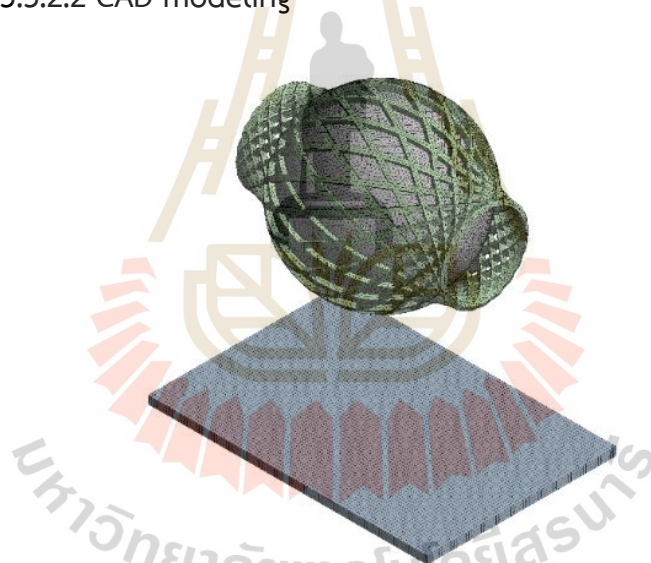


Figure 3.18 CAD model guava with expanded polyethylene cushion foam net

Simplifications and Assumptions

Several simplifications and assumptions were employed to facilitate the modeling process without compromising the essential mechanical behavior as shown in Figure 3.19

Guava Geometry: The natural irregularities of guava surfaces were neglected, and the fruit was modeled as a perfect sphere.

Foam Net Structure: The foam net was represented as a regular lattice of uniform cells, ignoring minor manufacturing imperfections.

Material Homogeneity: Both the EPE (Figure 3.20) and NRLF nets were assumed to be homogeneous and isotropic in their respective material properties.

Boundary Contact: The net was modeled to conform tightly to the guava surface, assuming perfect contact without significant gaps or slack.

Symmetry: Symmetry considerations were used wherever possible to reduce the computational domain and simulation complexity.

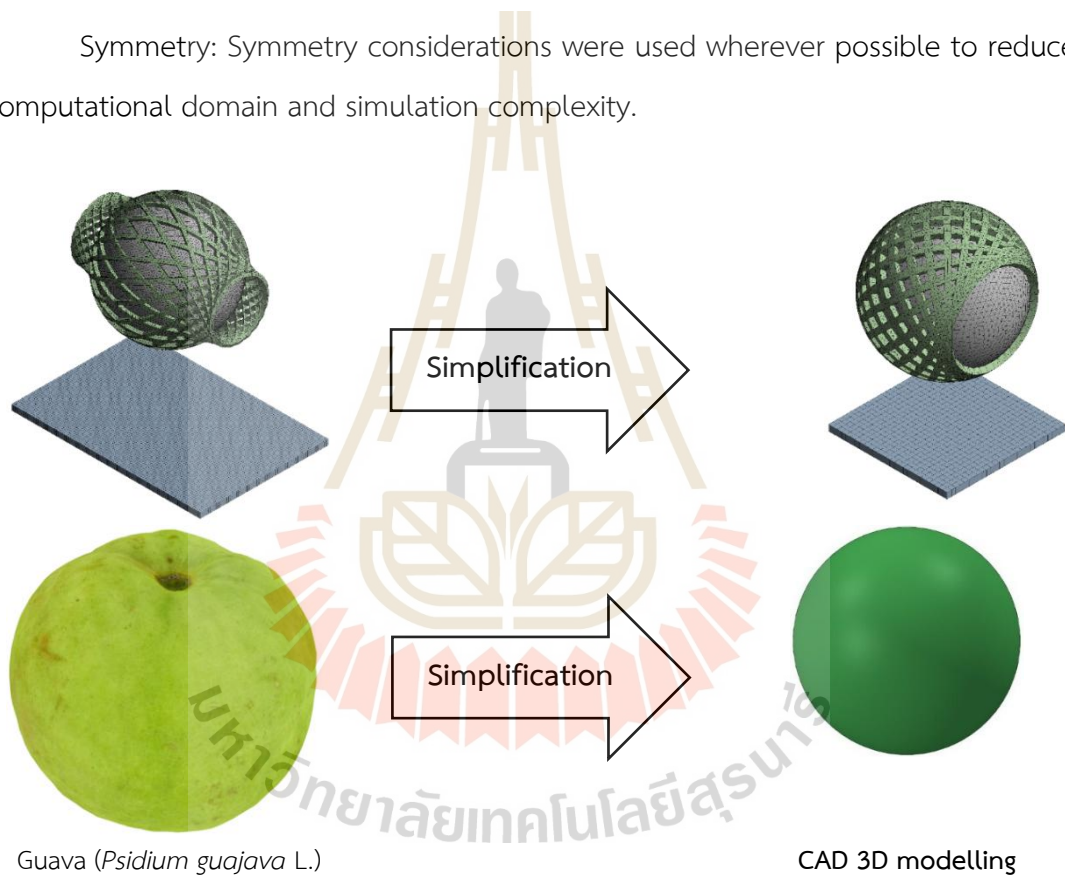


Figure 3.19 Simplifications of simulation model

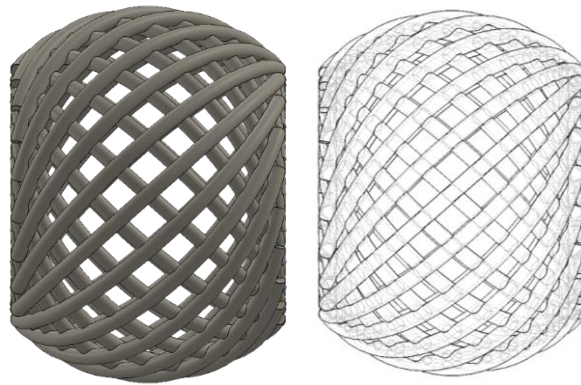


Figure 3.20 3D model of commercial cushion foam net

Parameter design of cushion net foam

Accurate parameter design is essential for optimizing the protective performance of cushioning systems. This chapter presents a comprehensive study on the parameterization and finite element method (FEM) simulation of Natural Rubber Latex Foam (NRLF) net structures intended for guava impact protection. The analysis investigates the effects of three principal parameters on the cushioning efficiency: filament diameter, filament number, and foam density. Three levels of filament diameter 2.5 mm, 3.5 mm, and 4.5 mm were considered, along with filament numbers of 15, 20, and 25 arranged across the net structure. Foam densities of 345 kg/m³, 397 kg/m³, and 420 kg/m³ were also examined to assess their influence on mechanical behavior.

CAD models corresponding to different filament numbers (15, 20, and 25) with a constant filament diameter of 3.5 mm were developed, as illustrated in Figure 3.21.




CAD Model			
Filaments number	15	20	25

Figure 3.21 CAD 3D model filament dimension 3.5 mm (number a:25, b: 20, and c: 15 filament)

3.3.2.3 Boundary Conditions (BCs)

Establishing appropriate boundary conditions (BCs) is crucial for accurately simulating the mechanical response of a guava fruit enclosed within cushioning packaging during impact scenarios. In this study, the guava, encased within either a commercial expanded polyethylene (EPE) net (Figure 3.22) or a Natural Rubber Latex Foam (NRLF) net, was modeled as undergoing free fall under the influence of gravitational acceleration. The simulation setup reflects a drop impact where the fruit-packaging assembly falls freely and strikes a rigid surface. To represent the ground contact, a planar fixed support was defined, constraining all translational and rotational degrees of freedom. Gravitational force was applied uniformly to the entire assembly to replicate natural free-fall conditions Table 3.4. These Material Definitions setting show in Table 3.5 and boundary conditions were carefully designed to mirror experimental setups commonly used in drop impact testing and to ensure realistic energy transfer and stress development upon collision.

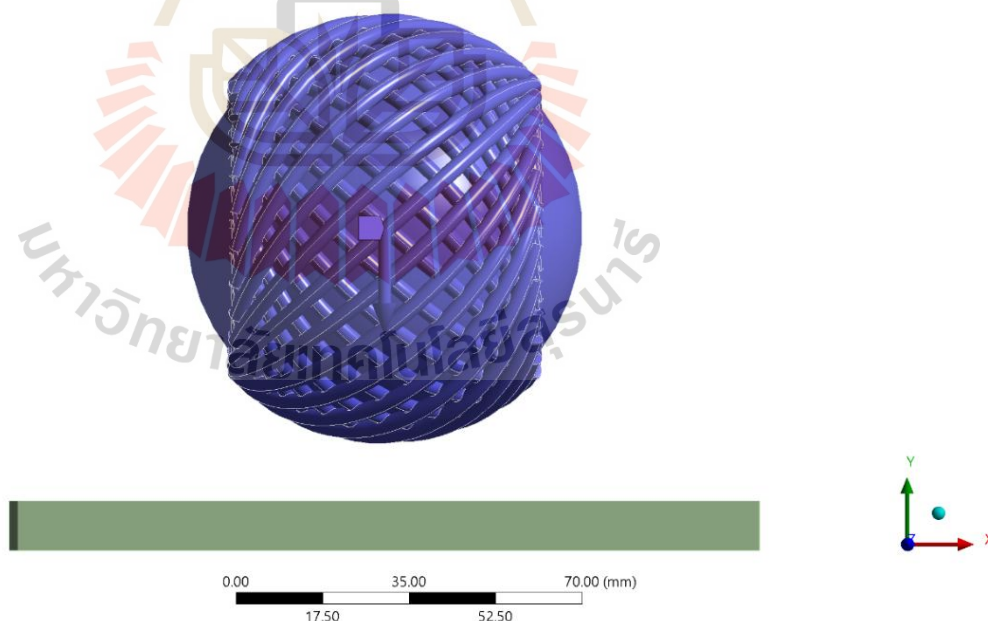


Figure 3.22 FEM model for simulating with the impact plane drop test.

Standard earth gravity direction at Drop height

$$mgh_1 = \frac{mv_1^2}{2} = mgh_2 = \frac{mv_2^2}{2} \quad (29)$$

The velocity calculated with $v_2 = \sqrt{2g(h_1 - h_2)}$

Table 3.4 Direction of setting standard earth gravity

Direction	Gravity
X component	0.00 mm/s ²
Y component	-9806.60 mm/s ²
Z component	0.00 mm/s ²

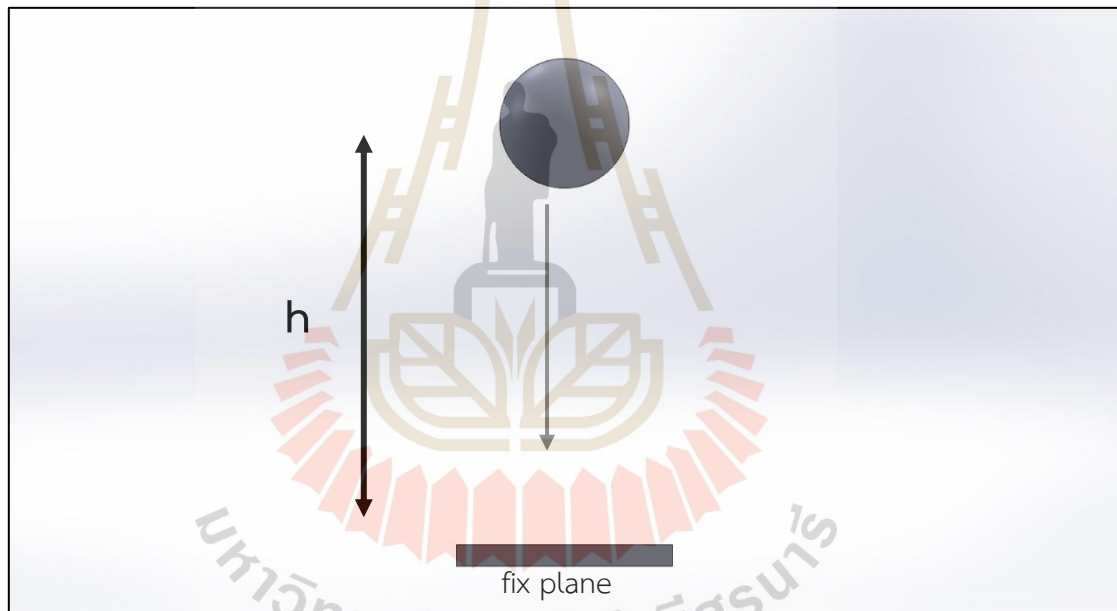


Figure 3.23 FEM model boundary conditions drop high setting

3.3.2.4 Material Definition

Table 3.5 Material parameters

Sample	Density ρ (Kg/m ³)	Compressive stress (kPa)	Young's modulus Y , (KPa)	Poisson's ratio ν
EPE	118.000	20.130	39.977	0.330
NRLF	272.060	56.850	105.482	0.330
Guava	1240.000	53.530	29.739	0.490

3.3.2.5 Mesh

Mesh generation represents a fundamental step in finite element analysis (FEA), directly influencing the accuracy, stability, and computational efficiency of the simulation. In this study, a high-quality mesh was developed for the guava and cushioning net assemblies to ensure reliable prediction of mechanical responses during drop impact events. The meshing strategy involved the use of tetrahedral elements for complex geometries, with refinement applied to critical regions such as the contact interfaces between the guava and the foam net, and the areas anticipated to experience high stress concentrations. Mesh sensitivity analyses were performed to determine an optimal balance between solution accuracy and computational cost. Appropriate element sizing, and convergence criteria were established to guarantee the numerical stability of the simulation results. This meshing approach aimed to faithfully capture deformation, stress distribution, and contact behavior under dynamic loading conditions. **Error! Reference source not found.** shown the finite element model d eveloped for the simulations. the meshing methods and assigned element sizes for each component, are summarized in Table 3.6.

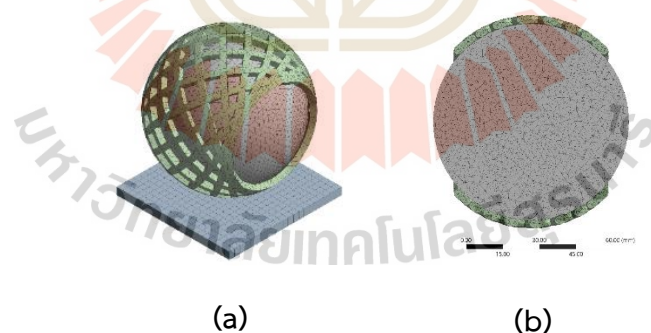


Figure 3.24 Finite element model (a) reverse-engineered guava cushion foam net model, outer mesh structure, (b) inner mesh structure)

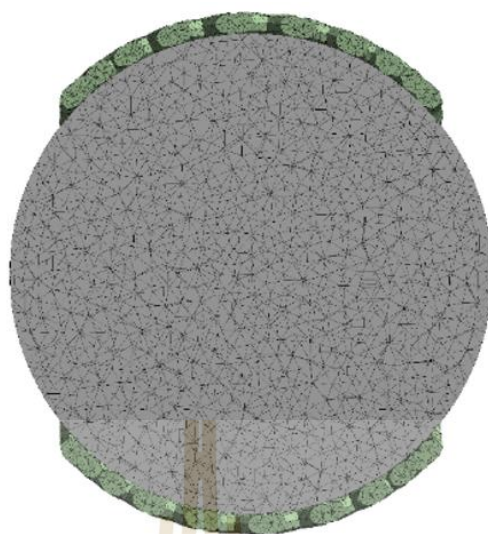


Figure 3.25 Show cross section in meshing setup of EPE cushion net foam 3.5X25 mm and guava mesh size 3.00mm

Table 3.6 Mesh method and element size

Body	Method	Element size(mm.)
Net foam	Tetrahedrons	3.00
Guava	Tetrahedrons	3.00
Impact plane	Hex Dominant	5.00

3.3.2.6 Mesh Convergence

In finite element analysis (FEA), *convergence* refers to the process of achieving a numerical solution that approximates the exact solution of the governing partial differential equations (PDEs) as the discretization of the spatial domain becomes increasingly refined (Zienkiewicz and Taylor, 2005). Mesh convergence is typically carried out by decreasing the element size and observing the effects on the solution's accuracy.

Finer mesh resolutions allow for a more accurate representation of the physical behavior across the domain, as they sample the geometry more thoroughly. However, increased accuracy often results in significantly higher computational costs, including greater memory usage and longer simulation runtimes (Cook et al., 2002). As

such, mesh convergence studies are essential for determining an appropriate balance between computational efficiency and solution accuracy (Bathe, 1996).

This FEM simulation investigates the effect of element size on the accuracy of stress predictions. The goal is to determine an optimal element size that minimizes the difference between the solution stress and the stress obtained from a finer mesh. The target is to achieve a stress difference of less than 5% shown in Figure 3.27 compared to the finer mesh solution. However, the global edge length in the current mesh is already smaller than 4.00 mm. This model uses NRLF foam net study 3.5mm 25x25, the statistics shown in

Figure 3.26 . sensitivity analysis test statistics shown in Figure 3.27.

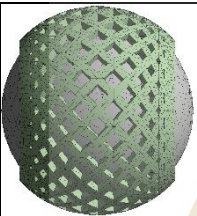
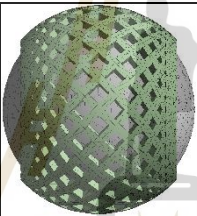
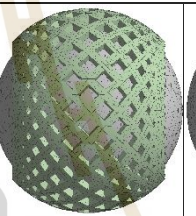
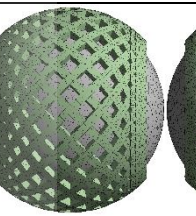
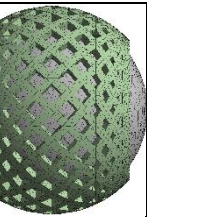
Model					
Mesh size	7.0mm.	6.0 mm.	5.0 mm.	4.0 mm.	3.0 mm.
Nodes	11287	10798	16449	20896	35584
Elements	20908	25278	28382	33061	51891

Figure 3.26 Effect of mesh size, Nodes, and elements on CAD model of NRLF cushion net foam 3.5 mm 25x25

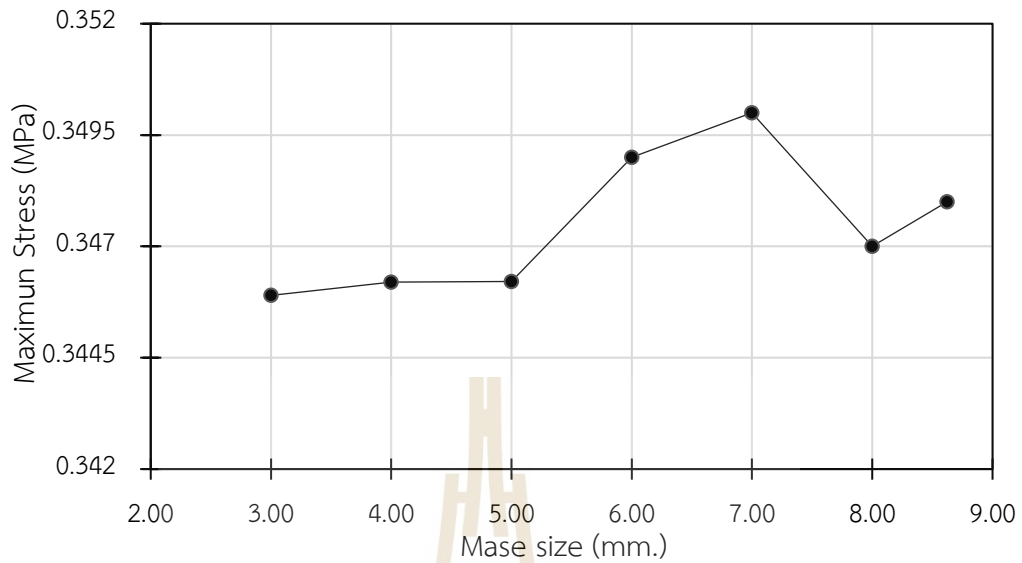


Figure 3.27 Mesh sensitivity analysis

3.3.2.7 Convergence rate

To investigate the effect of mesh refinement on the model's accuracy and computational efficiency, presents a summary of element sizes used in the NRLF net foam model with a 3.5 mm filament diameter and a 25 × 25 arrangement. As the element size is gradually reduced, the number of elements and nodes increases, leading to finer mesh resolution and a better approximation of the geometry and stress distribution. However, this increase in resolution also results in higher computational demands. The selected element size of 3.0- 4.0 mm represented an optimal balance between accuracy and computational feasibility for the simulation.

3.3.2.8 Controlling discretization error

Convergence error

$$\text{Convergence error} = \left| \frac{\text{result}(n) - \text{result}(n-1)}{\text{result}(n)} \right| \quad (30)$$

Solution error

$$\text{Solution error} = \left| \frac{\text{FE result} - \text{asymptotic result}}{\text{FE result}} \right| \quad (31)$$

Tabel 3.7 Mesh convergence

Mesh size	Elements	Nodes	Convergence error
7.0	20908	11287	-
6.0	25278	10798	33%
5.0	28382	16449	25%
4.0	33061	20896	13%
3.0	51891	35584	4%

3.4 Validation

To validate the predictive accuracy of the developed finite element model (FEM) shown in Figure 3.29, the simulated bruise areas were compared against experimental results obtained from drop tests of guava fruits without any cushioning material. The experimental data were adapted from the study by (Saengwong-Ngam et al. 2024), which evaluated the impact protection performance of natural rubber latex foam composites reinforced with bamboo leaf fiber. The experimental procedure involved dropping the fruits from heights of 200 mm, 300 mm, and 400 mm shown in

Figure 3.28 after four days of storage, with the resulting bruise areas measured as 111.7 mm², 150.1 mm², and 216.4 mm², respectively. The FEM was constructed to replicate the experimental conditions precisely, simulating the free-fall impact of the guava fruits onto a rigid surface without protective cushioning. The comparison of the experimental and simulated bruise areas is presented in drop test simulation. Drop test simulation setup

Table 3.8 Material properties for the drop test simulation analysis

Component	Modulus of Elasticity, E (MPa)	Poisson's ratio	Mass (g)
Stainless -steel ball	200000	0.31	250
Guava	0.105	0.33	250
Plane	200000	0.30	2077.2

The entire computational domain consisted of 4,565 nodes and 22,154 elements. A Tetrahedron mesh was employed for all components to ensure accurate capture of contact interactions and deformation behavior. The mesh sizing was assigned as follows: 6 mm for the stainless-steel ball, 8 mm for the plane beneath the guava, and 10 mm

The stainless-steel ball and the guava were initially positioned above the plane at a specified drop height. Both components were assigned an initial velocity of zero prior to release, with gravitational acceleration applied uniformly in the negative y-axis direction to simulate free-fall motion.

The bottom surface of the supporting plane was fully constrained in all translational degrees of freedom (fixed support) to prevent any movement during the impact event.

No constraints were imposed on the stainless-steel ball or the guava in order to allow free motion until contact initiation occurred.

An explicit dynamic analysis was employed due to the highly nonlinear behavior associated with impact events and large deformation responses, particularly in the guava specimen, which exhibited low stiffness and viscoelastic-like characteristics.

This boundary condition setup ensured that the simulation closely represented the experimental setup used for validation, thereby enabling a direct comparison between simulated and observed deformation behaviors under drop test conditions.

Table 3.9 The entire computational domain consisted of 4,565 nodes and 22,154 elements. A Tetrahedron mesh was employed for all components to ensure accurate capture of contact interactions and deformation behavior. The mesh sizing was assigned as follows: 6 mm for the stainless-steel ball, 8 mm for the plane beneath the guava, and 10 mm

The stainless-steel ball and the guava were initially positioned above the plane at a specified drop height. Both components were assigned an initial velocity of zero prior to release, with gravitational acceleration applied uniformly in the negative y-axis direction to simulate free-fall motion. The bottom surface of the supporting plane was fully constrained in all translational degrees of freedom (fixed support) to prevent any movement during the impact event. No constraints were imposed on the stainless-steel ball or the guava in order to allow free motion until contact initiation occurred.

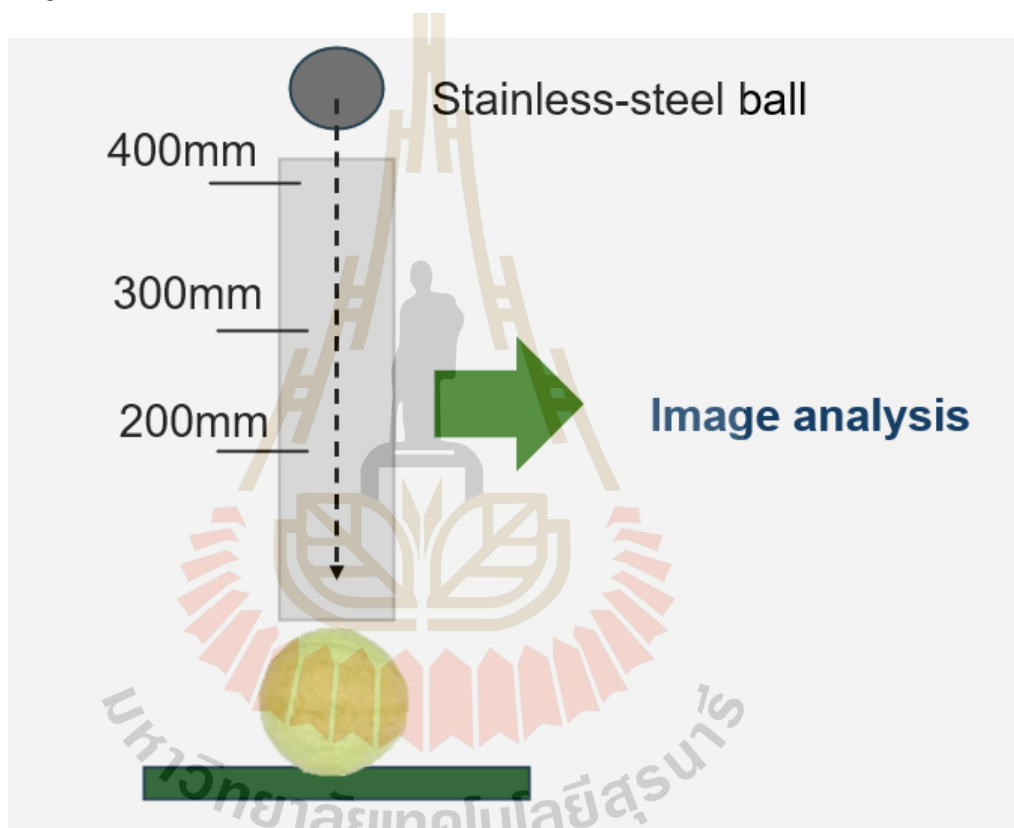


Figure 3.28 The experimental fruit bruise damage

3.4.1. Boundary Conditions Setting for Validation of Drop Test Model

In the finite element simulation of the drop test validation, appropriate boundary conditions were defined to accurately replicate the physical behavior of the system during impact. The model comprised three primary components: a stainless-steel ball, a guava specimen, and a supporting plane, each characterized by specific material properties as summarized in Table 3.8

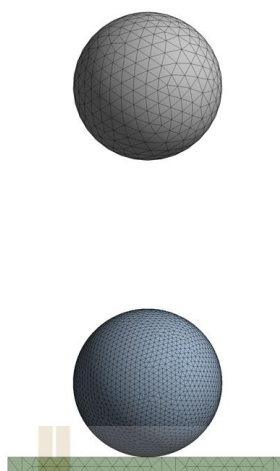


Figure 3.29 Validation model using FEM Drop test simulation setup

Table 3.8 Material properties for the drop test simulation analysis

Component	Modulus of Elasticity, E (MPa)	Poisson's ratio	Mass (g)
Stainless -steel ball	200000	0.31	250
Guava	0.105	0.33	250
Plane	200000	0.30	2077.2

The entire computational domain consisted of 4,565 nodes and 22,154 elements. A Tetrahedron mesh was employed for all components to ensure accurate capture of contact interactions and deformation behavior. The mesh sizing was assigned as follows: 6 mm for the stainless-steel ball, 8 mm for the plane beneath the guava, and 10 mm

The stainless-steel ball and the guava were initially positioned above the plane at a specified drop height. Both components were assigned an initial velocity of zero prior to release, with gravitational acceleration applied uniformly in the negative y-axis direction to simulate free-fall motion.

The bottom surface of the supporting plane was fully constrained in all translational degrees of freedom (fixed support) to prevent any movement during the impact event.

No constraints were imposed on the stainless-steel ball or the guava in order to allow free motion until contact initiation occurred.

An explicit dynamic analysis was employed due to the highly nonlinear behavior associated with impact events and large deformation responses, particularly in the guava specimen, which exhibited low stiffness and viscoelastic-like characteristics.

This boundary condition setup ensured that the simulation closely represented the experimental setup used for validation, thereby enabling a direct comparison between simulated and observed deformation behaviors under drop test conditions.

Table 3.9 Comparison of experimental and simulated bruise areas

Drop Height (mm)	Experimental Bruise Area (mm ²)	Simulated	
		Surface displacement (mm ²)	Different (%)
200	111.7	107.9	3.5
300	150.1	146.8	2.4
400	216.4	209.7	3.2

Despite these errors, the study concludes that the FEM model successfully captured the general trend of increasing bruise area with greater drop heights. This means that while the exact numerical values might have discrepancies, the model correctly predicted that higher drops would lead to larger bruise areas, which is a crucial aspect of its predictive capability.

The results confirm that the finite element model is capable of reasonably predicting the impact-induced damage behavior of guava fruits under free-fall conditions without cushioning. This validation is significant because it establishes the model as a reliable tool for further research. Consequently, the validated model can now be utilized

for further simulations involving the application of protective cushioning materials. This implies that researchers can use this model to virtually test different cushioning designs and materials to reduce impact damage, saving time and resources that would otherwise be spent on physical experiments.



CHAPTER IV

RESULTS AND DISCUSSION

4.1 Introduction

This chapter presents a comprehensive analysis of the finite element method (FEM) simulations conducted to evaluate the protective performance of Natural Rubber Latex Foam (NRLF) nets for guava during drop-impact scenarios. The study focuses on three primary methodologies for stress analysis.

The maximum equivalent (von Mises) stress was quantified to determine the peak mechanical loads on the fruit tissue. This analysis was performed during drop tests conducted at a height of 200 mm for parameter design investigations and 100 mm for density reduction investigations.

The investigation focuses on three critical parameters

Filament diameter (2.5, 3.5, and 4.5 mm)

Filament number (15, 20, and 25 filaments)

Foam density (345, 397, and 420 kg/m³)

4.2 Parameter variation and result

This simulation utilizes the Finite Element Method (FEM) to analyze the performance of eco-friendly foam nets for guava protection during high-impact freefall drops (200 mm). The study compares two cushion materials: expanded polyethylene (EPE) foam, a popular choice for cushioning and packaging, and a new, eco-friendly alternative made from natural rubber foam latex. The goal is to optimize the design of the foam net for guava protection by evaluating the damage caused by the external

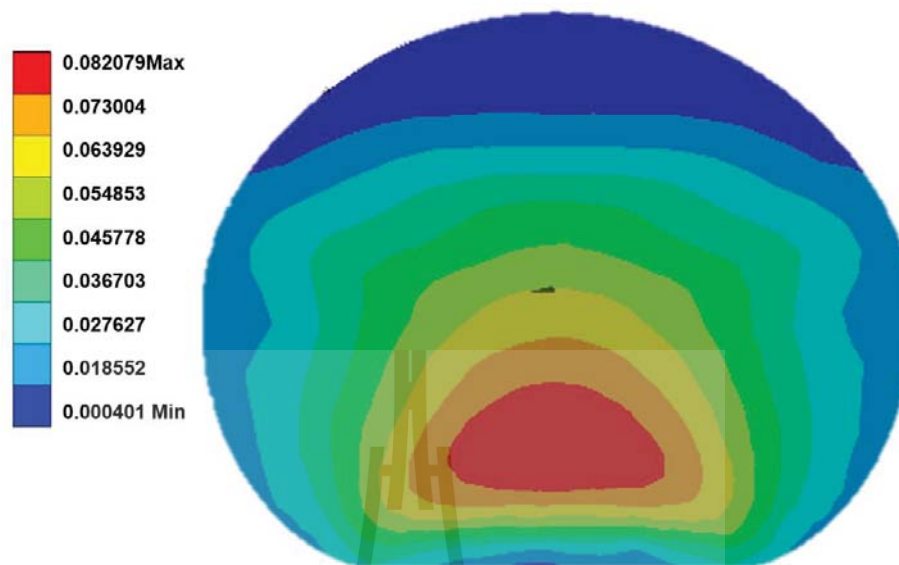
force exerted during the freefall drop. This optimization focuses on the size and number of filaments within the foam net.

EPE commercial cushions performance.

The finite element simulations conducted in this study demonstrate that the application of a commercial Expanded Polyethylene (EPE) foam cushion effectively reduces the peak stress experienced by guava fruits during drop impact compared to unpackaged conditions, as illustrated in Figure 4.1. Specifically, the maximum equivalent stress observed in the unpackaged guava was approximately 0.0821 MPa, whereas the guava cushioned with EPE foam exhibited a reduced peak stress of approximately 0.0774 MPa (Figure 4.3), representing a decrease of about 5.7%. This reduction indicates that the EPE foam is capable of partially absorbing and redistributing the impact energy, thereby mitigating the severity of localized stresses within the guava tissue.

The stress-time presented in Figure 4.2 further reveals that the peak stress occurs at approximately 0.016 seconds after impact, corresponding to the moment of maximum deformation, followed by a rapid stress decay, which is characteristic of elastic recovery behavior post-impact. Moreover, the comparison of stress distribution patterns between the two cases shows that while unpackaged guava suffered from concentrated stress regions (Figure 4.1a), the cushioned specimen displayed a more diffused stress field (Figure 4.1b), further corroborating the role of the foam in impact energy dispersion. While EPE foam demonstrated measurable stress attenuation, the comparatively modest degree of stress reduction indicates that its cushioning performance could be limited, especially for highly delicate fruits or at greater drop heights.

(a)



(b)

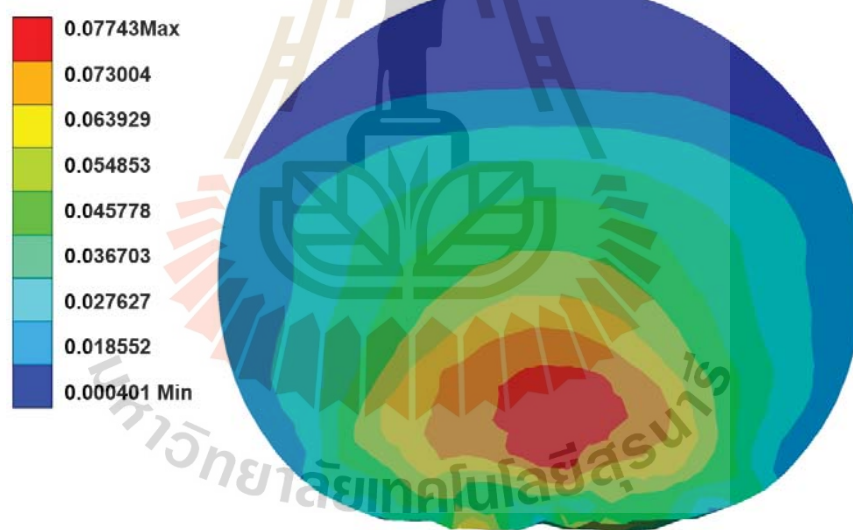


Figure 4.1 Stress [MPa] in the gravity direction for the drop height 200 mm model (a) guava unpacking (b) guava with EPE commercial cushion

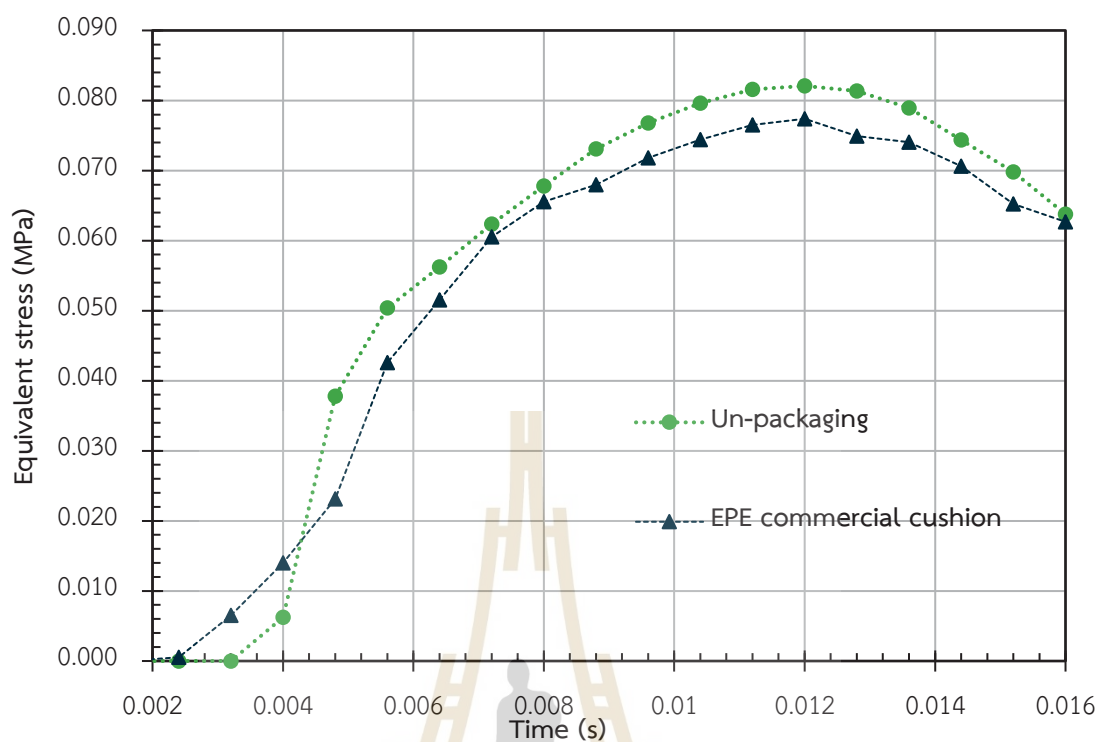


Figure 4.2 Maximum von-miss equivalent stress of guava and time at 0.016 s. drop height of 200 mm.

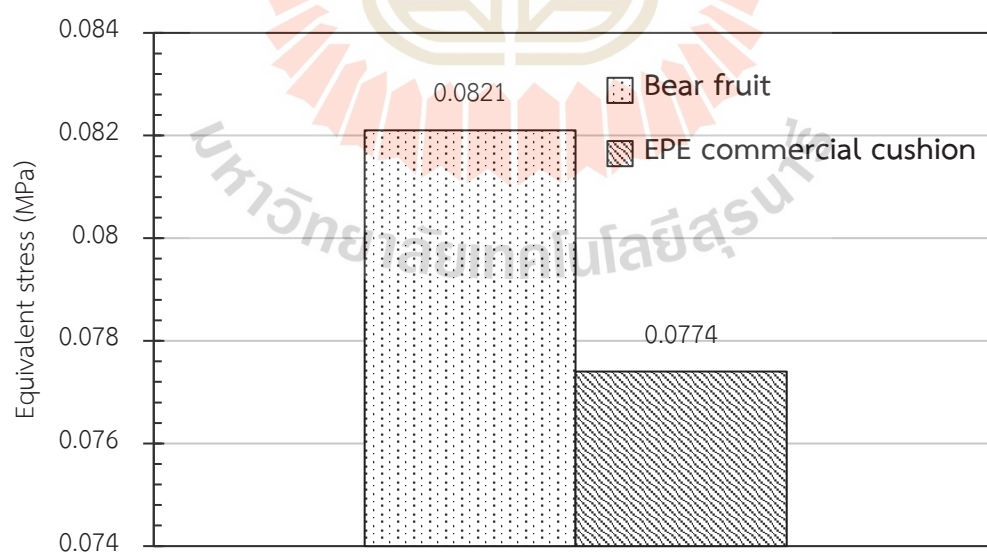
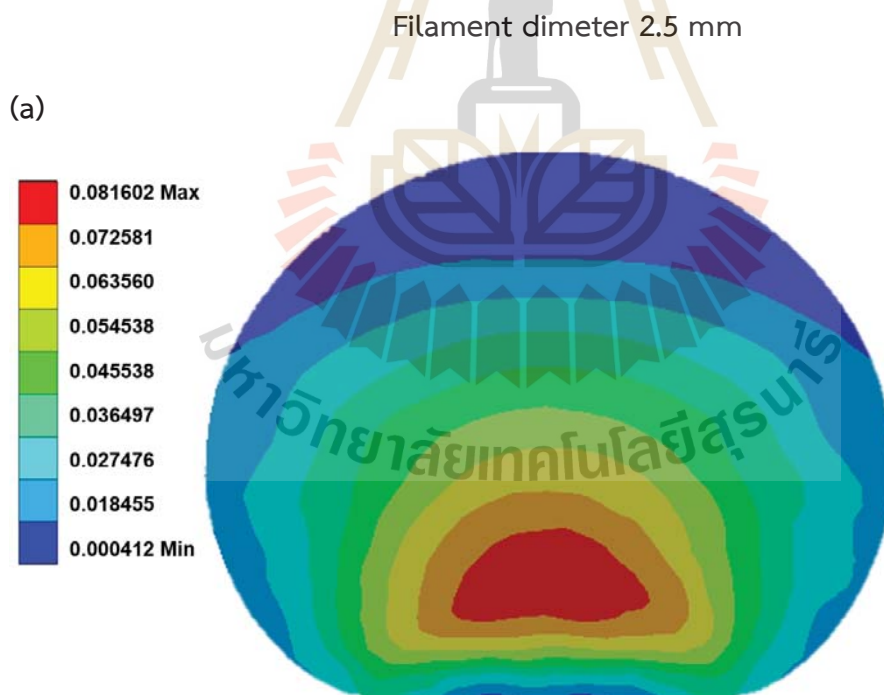


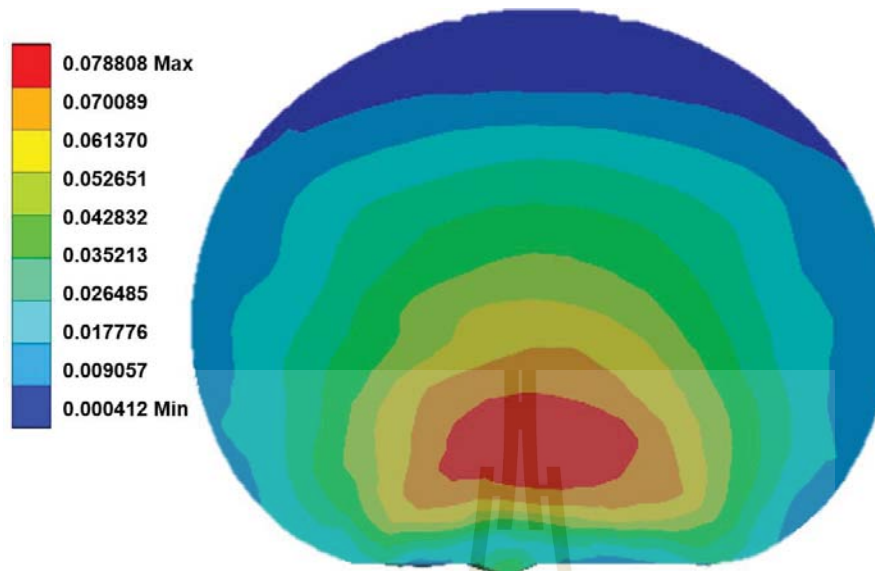
Figure 4.3 Maximum (von-miss) drop test of guava bear fruit compared to EPE commercial cushion foam net.

4.3 Effect of size and number on cushion performance.

The performance of cushioning materials is heavily influenced by both the size and the number of constituent elements within the foam net structure. In this study, the impact of varying the filament size and number of filaments on the protective behavior of the NRLF cushion net was investigated under drop impact scenarios. Larger filaments and higher filaments number typically result in greater energy absorption capacity, potentially enhancing the cushioning effect. The investigation explores how these parameters influence the maximum stress and strain experienced by the guava fruit, providing valuable insights into optimizing the design of foam net cushioning for efficient fruit protection. By systematically varying the size and number of filaments, this study aims to determine the optimal combination that balances performance and material efficiency in preventing damage during drop events.



(b)



(c)

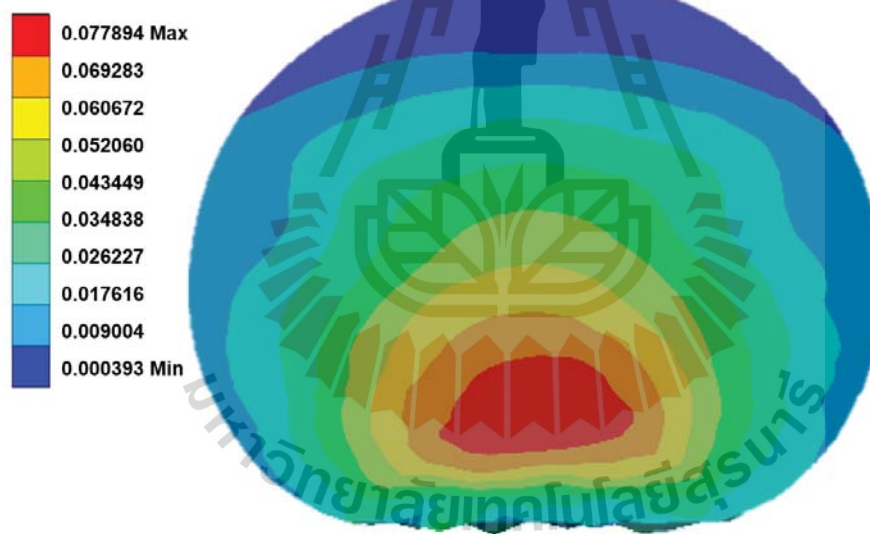


Figure 4.4 Stress in the gravity direction for the drop height model (a) NRLF 2.5x15, (b) NRLF 2.5x20 and (c) NRLF 2.5x25 from a cross-section view.

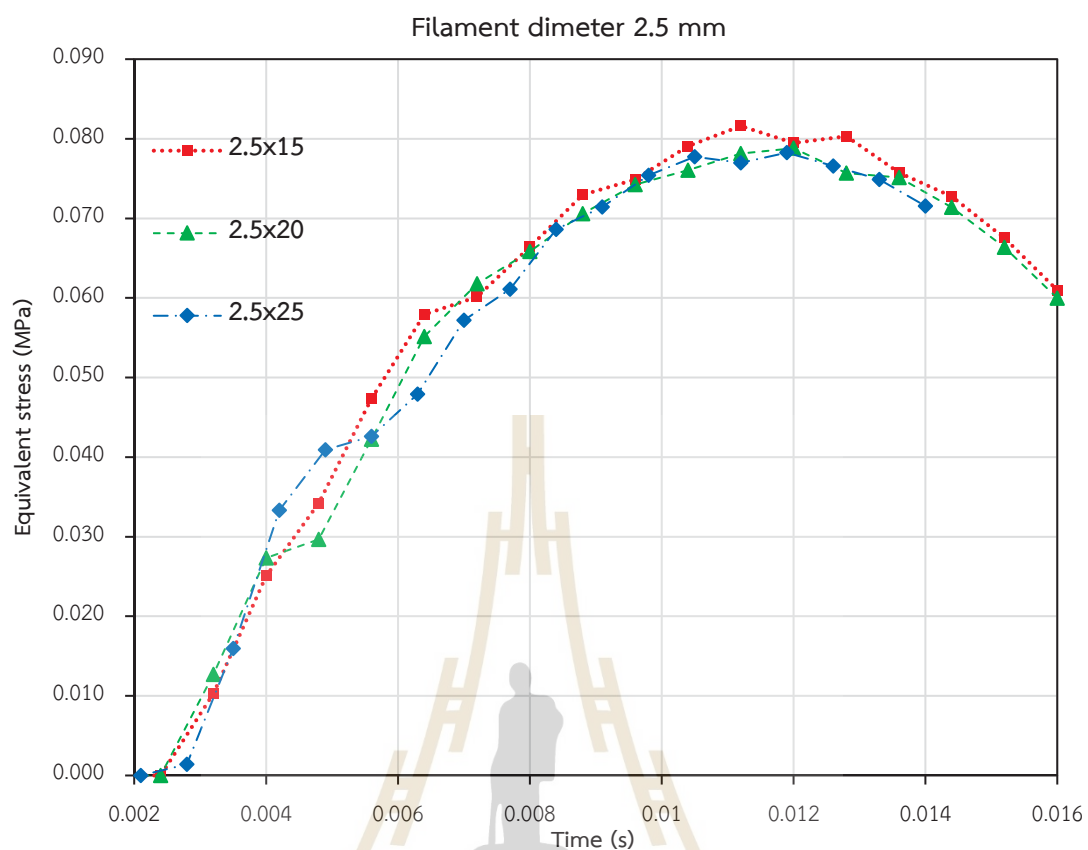
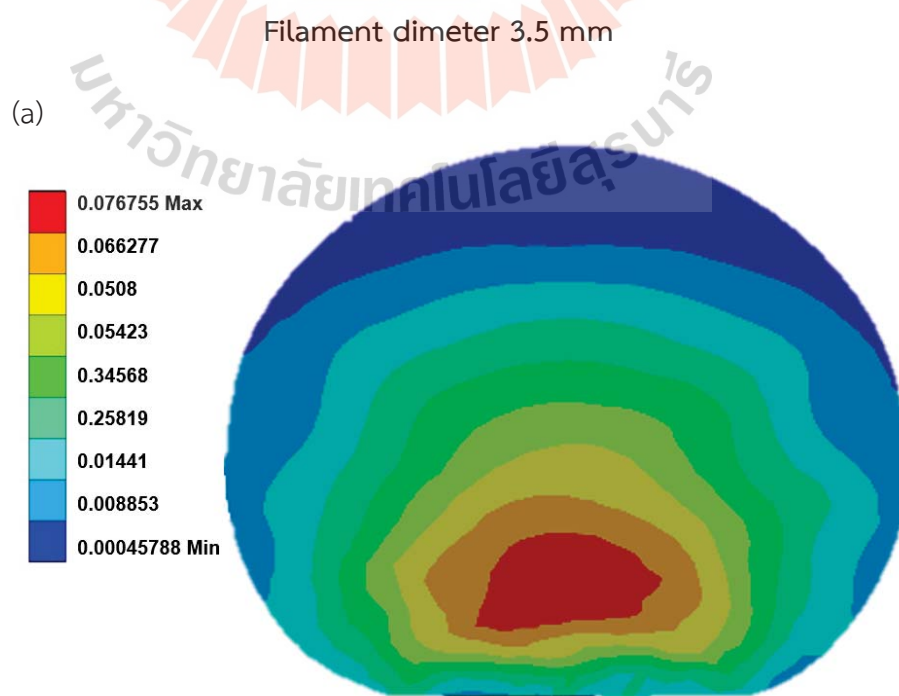
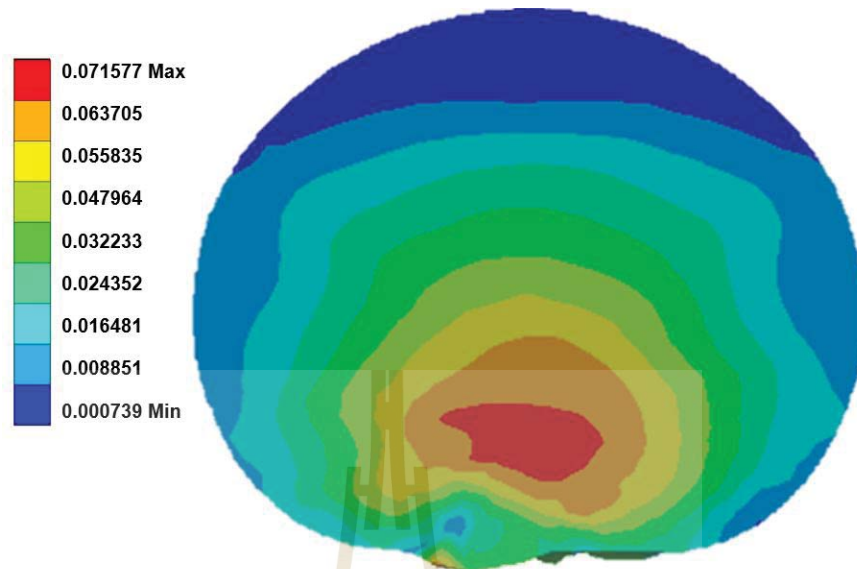


Figure 4.5 Stress distribution plots in guava sample (max von-mises stress, [MPa]) of NRLF foam net diameter filament size 2.5 mm.



(b)



(c)

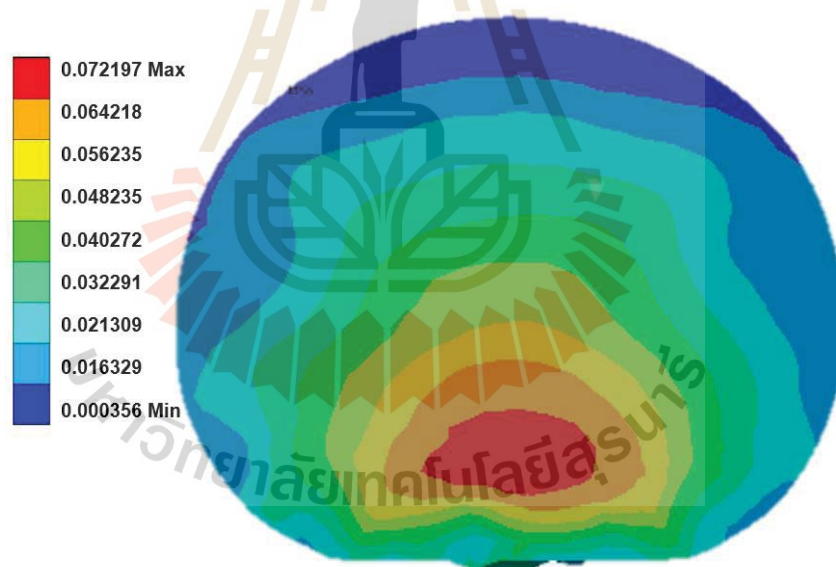


Figure 4.6 Stress [MPa] in the gravity direction for the drop height model (a) NRLF 3.5x15, (b) NRLF 3.5x20 and (c) NRLF 3.5x15 from a cross-section view show at time 0.0012 s.

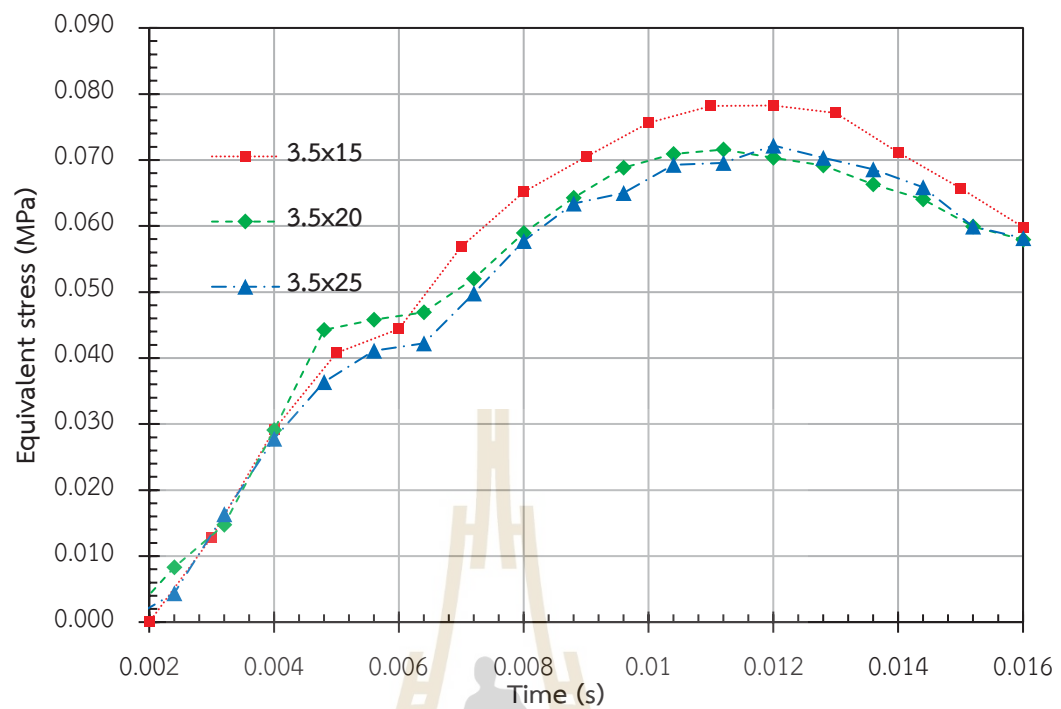
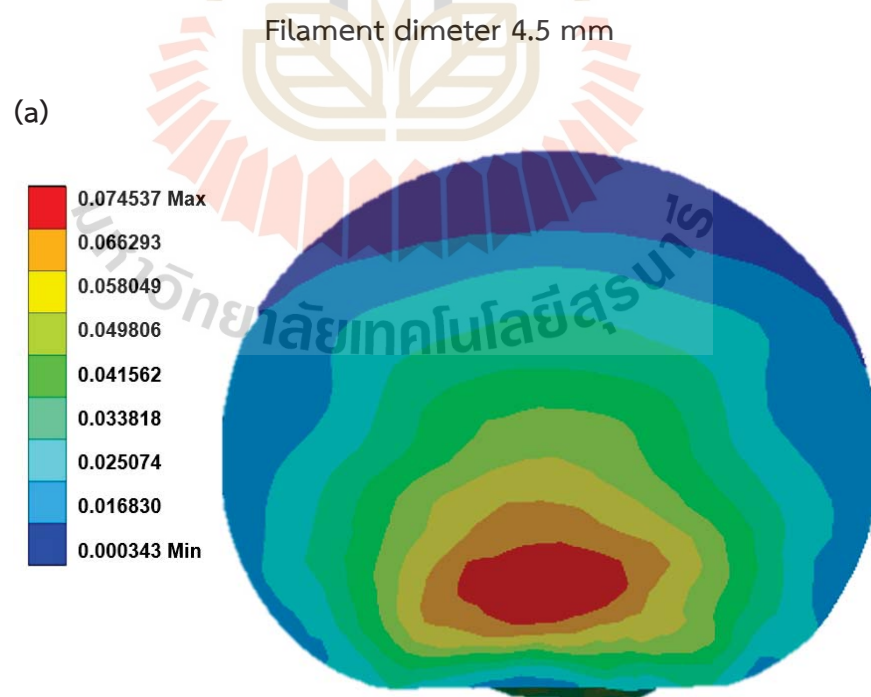
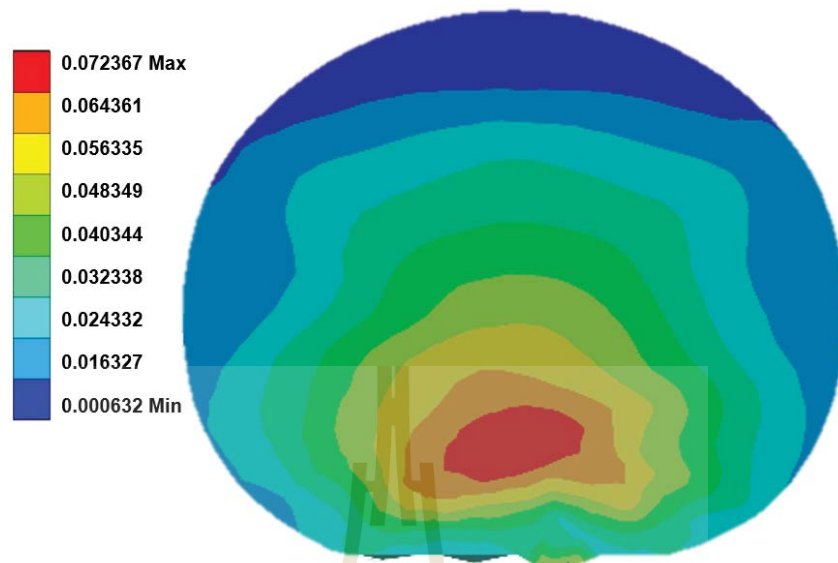


Figure 4.7 Stress distribution plots in guava sample (max von-mises stress, [MPa]) of NRLF foam net diameter filament size 3.5 mm.



(b)



(c)

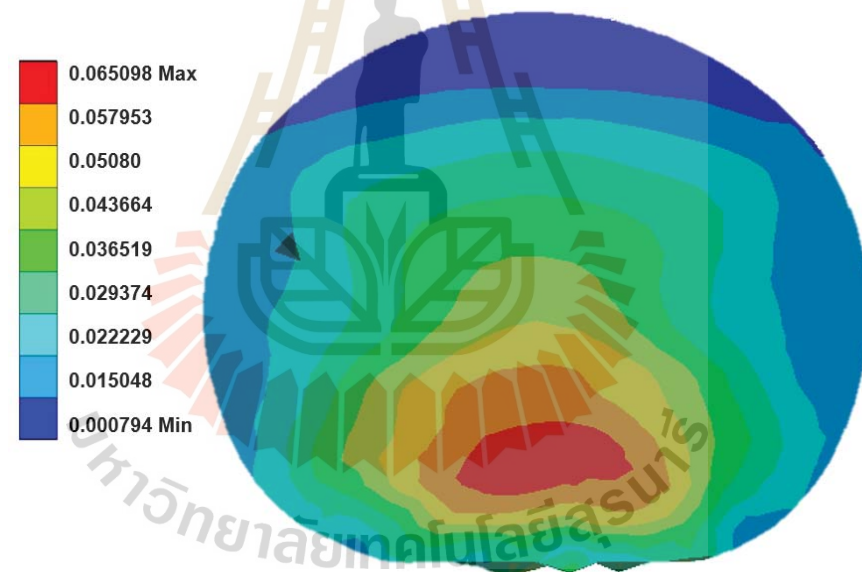


Figure 4.8 Stress [MPa] in the gravity direction for the drop height model (a) NRLF 4.5x15, (b) NRLF 4.5x20 and (c) NRLF 4.5x15 from a cross-section view show at time 0.0012 s.

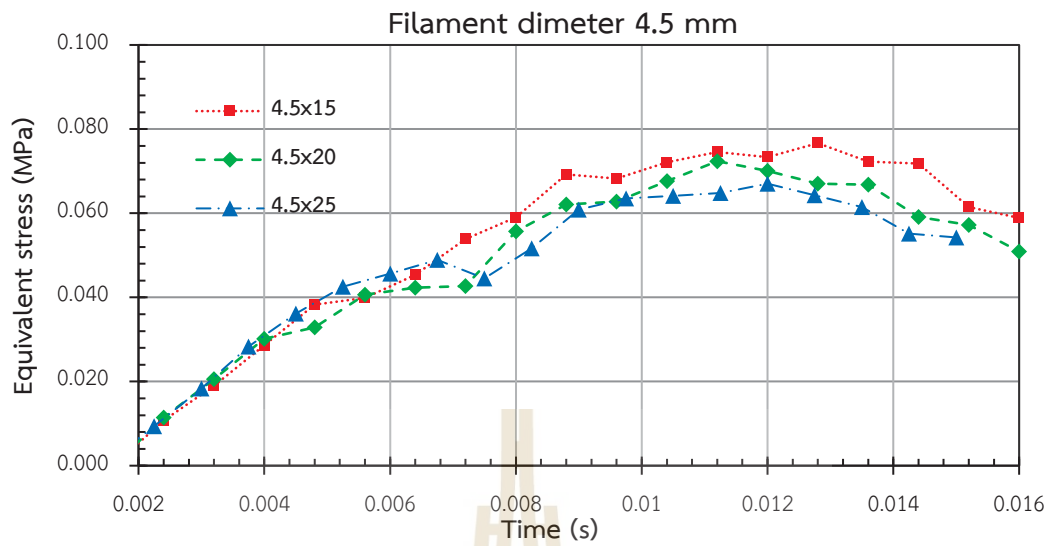


Figure 4.9 Stress distribution plots in guava sample (max von-mises stress, [MPa]) of NRLF foam net diameter filament size 4.5 mm.

Cushion performance results for NRLF 4.5x15 and EPE 3.5x25 cushions showed near-maximum stress. Increasing the number of filaments to 20 resulted in decreases of 5.9% and 7.0% in maximum stress, respectively.

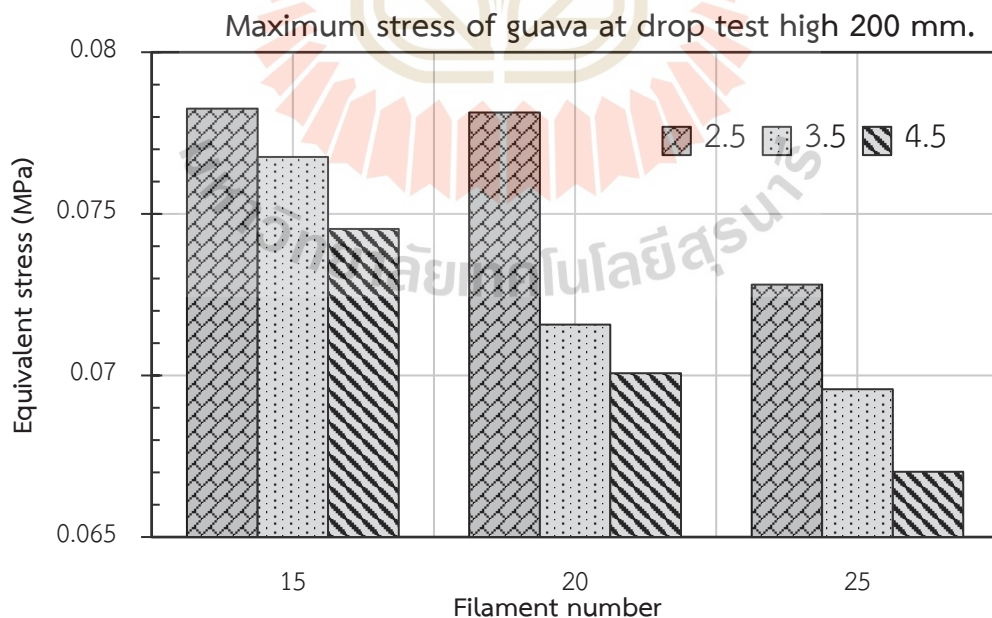


Figure 4.10 Maximum (von-miss) drop test of Guava NRLF packaging

The results from the drop test at a height of 200 mm Figure 4.11 show that the maximum equivalent stress experienced by the guava varied depending on the type and thickness of the cushioning material used. The unprotected guava (unpackaging condition) showed the highest equivalent stress, with a recorded value of 0.0821 MPa. This value serves as a baseline for comparison against other packaging configurations. When using filament materials of different thicknesses, a noticeable reduction in stress values was observed. The application of a 2.5 mm filament resulted in a stress value of 0.0728 MPa, indicating that even a relatively thin layer of cushioning can reduce the transmitted force to the fruit. Further improvement was seen with the 3.5 mm filament, which reduced the stress to 0.0696 MPa. The most significant decrease in stress was achieved with the 4.5 mm filament, which showed a value of 0.0670 MPa.

These findings suggest a trend in which increasing filament thickness corresponds with lower stress levels during impact. The data indicates that thicker cushioning layers are more effective at dissipating impact energy, thereby reducing the mechanical load transferred to the guava.

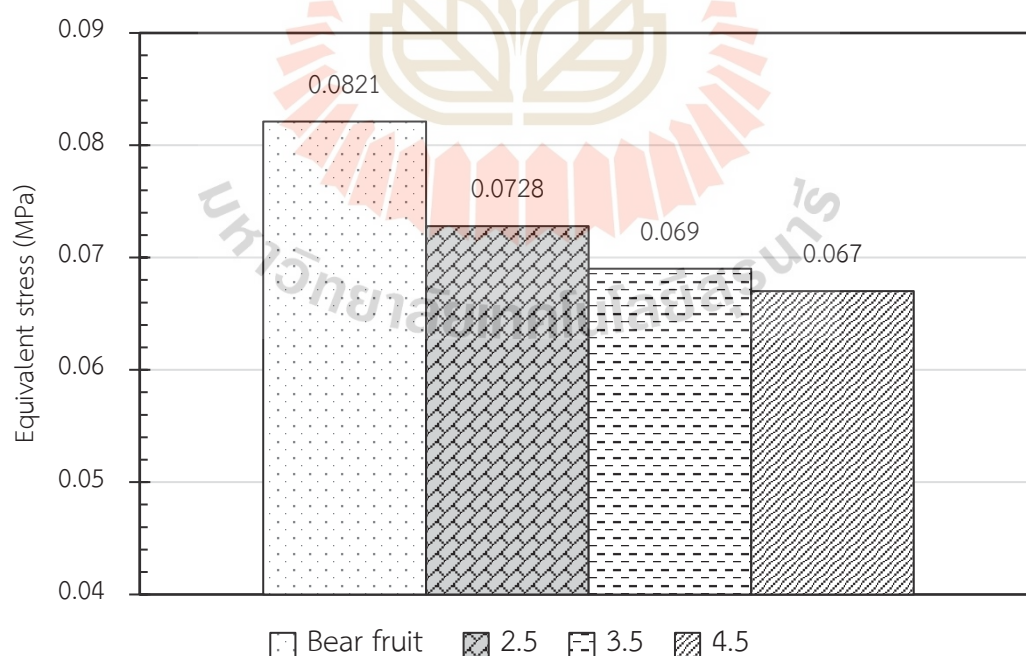


Figure 4.11 Maximum equivalent stress drop test 200 mm was observed at 0.013 s after impact and NRLF filament number 25.

Figure 4.12 Maximum equivalent stress drop test 200 mm was observed at 0.013 s after impact of bear fruit and EPE.

This study investigated the maximum equivalent stress experienced by guava during a drop test from a height of 200 mm under three different packaging conditions: no packaging, EPE commercial cushion, and NELF 4.5×25. The results revealed that the unprotected guava (no packaging) exhibited the highest stress value at 0.0821 MPa. When cushioned with the EPE commercial material, the stress was reduced to 0.0774 MPa, representing a 5.72% decrease. Notably, the NELF 4.5×25 material demonstrated the most effective cushioning performance, lowering the stress to 0.0670 MPa, which corresponds to a reduction of approximately 18.39% compared to the unpackaged case.

4.4 Density Reduction Effects on Impact Protection

This study investigates strategies to optimize the weight of NRLF by reducing its density while maintaining cushioning performance. Two primary approaches are examined: increasing internal voids within the foam (densities of 420, 397, and 345 kg/m³) to decrease overall weight, and reducing the number of cushion filaments (25, 20, and 15 filaments) used in the material. The research aims to identify the optimal balance between minimizing weight and preserving cushioning effectiveness. A Glom Sali guava

(250 g) investigation at drop test 100 mm. is used as a model fruit representing spherical produce.

The drop test simulation results show that both the density of the cushion material (420, 397, and 345 kg/m³) and the number of filaments (25, 20, and 15) significantly influenced the maximum stress experienced by the guava upon impact.

Across all densities, it was observed that a reduction in filament number consistently led to an increase in maximum stress. For example, at a density of 420 kg/m³, the maximum stress values for 25, 20, and 15 filaments were approximately 0.0566 MPa, 0.0580 MPa, and 0.0635 MPa, respectively. This trend persisted for the other densities: at 397 kg/m³, the stress increased from 0.0578 MPa (25 filaments) to 0.0640 MPa (15 filaments); and at 345 kg/m³, the stress rose from 0.0594 MPa (25 filaments) to 0.0653 MPa (15 filaments).

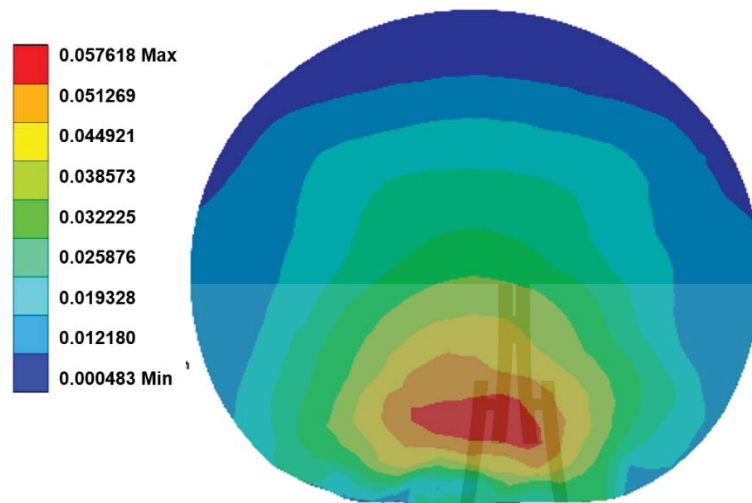
This pattern indicates that reducing the number of cushioning filaments diminishes the material's ability to absorb impact, regardless of density. Moreover, comparing across densities at the same filament count, lower density materials exhibited higher maximum stress. At 25 filaments, the maximum stress increased from 0.0566 MPa (420 kg/m³) to 0.0594 MPa (345 kg/m³), and a similar pattern was seen for filament numbers 20 and 15.

These results reflect the trade-off between weight reduction and cushioning performance. As both lower density and reduced filament count contribute to decreased material usage and lighter weight, they also compromise energy absorption capacity, leading to increased stress on the guava during impact.

The time of peak stress was observed at approximately 0.013 seconds after impact in all cases the result shown in Figure 4.22, which aligns with the expected moment of maximum deformation upon contact. This further confirms that the initial impact resistance is a critical factor in the effectiveness of the cushioning system.

filaments number 25.

(a)



(b)

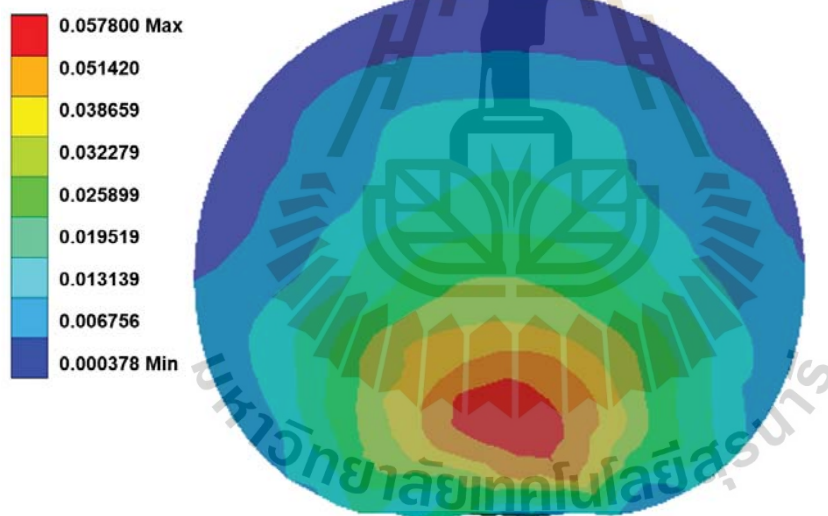


Figure 4.13 Stress [MPa] in the gravity direction for the drop height 100 mm filaments number 25 and the density (kg/m^3) (a) 420, and (b) 397 from a cross-section view.

(c)

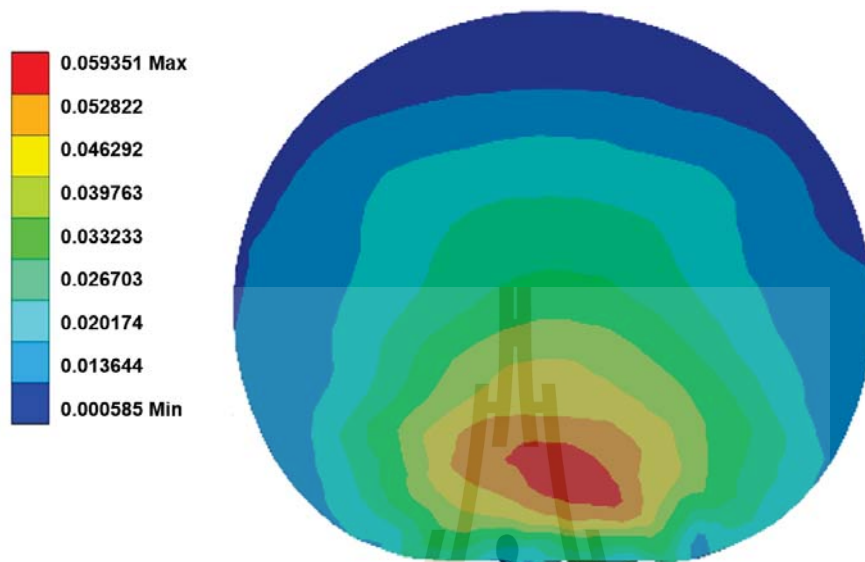


Figure 4.14 Stress [MPa] in the gravity direction for the drop height 100 mm filaments number 25 and the density (kg/m^3) (a) 420, (b) 397, and (c) 345 from a cross-section view.

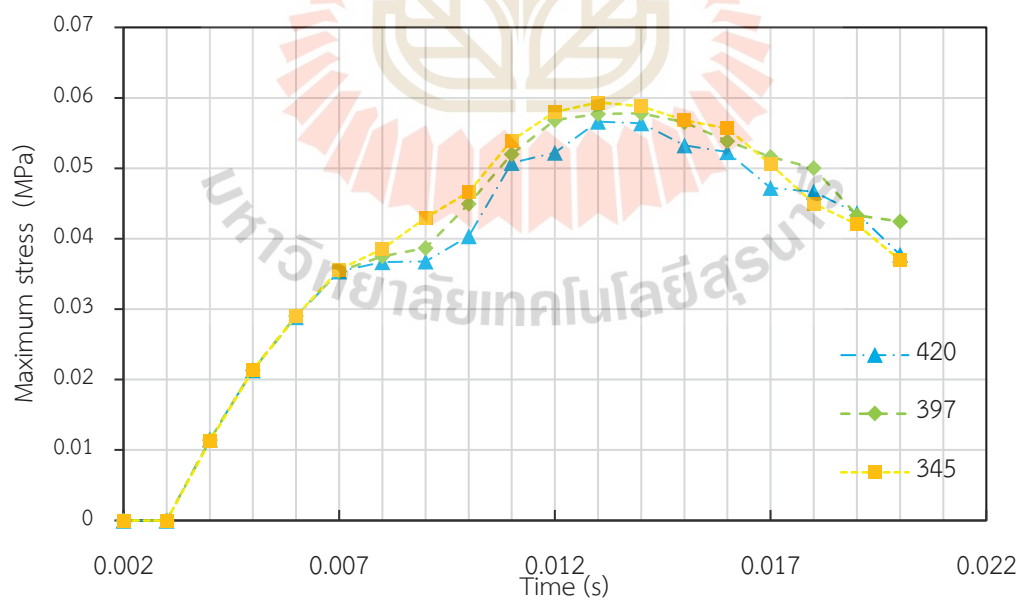


Figure 4.15 Plot Maximum stress (MPa) Time (s) plot for the model of filaments number 25 of and the density (kg/m^3) 420, 397, and 345.

filaments number 20.

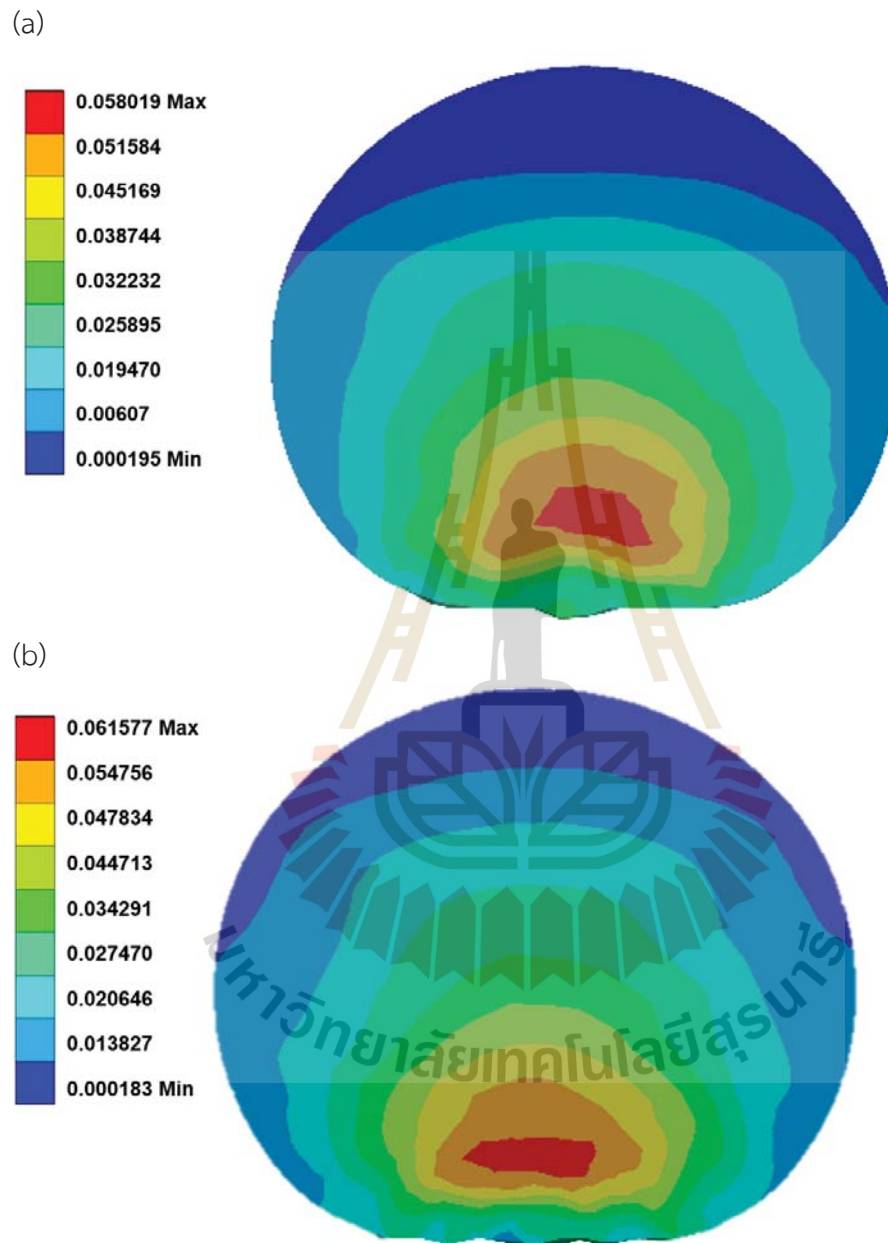


Figure 4.16 Stress in the gravity direction for the drop height 100 mm filaments number 20 and the density (kg/m^3) (a) 420, and (b) 397 from a cross-section view.

(c)

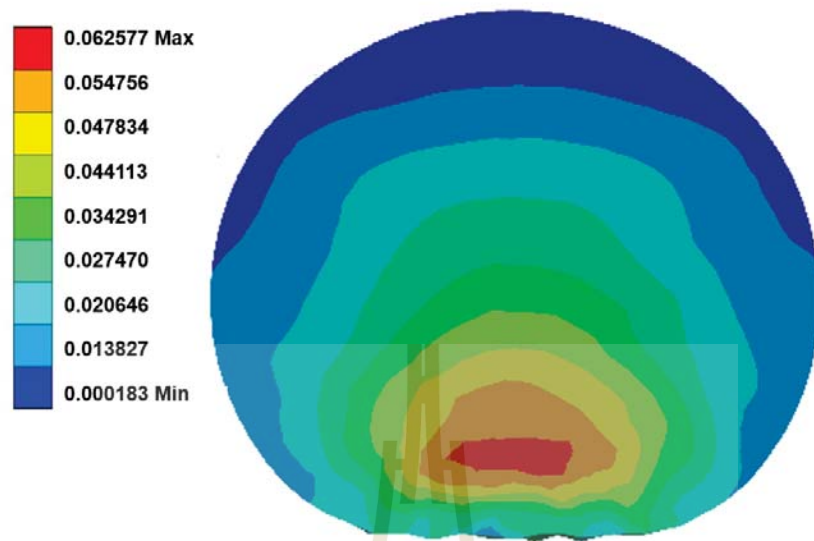


Figure 4.17 Stress in the gravity direction for the drop height 100 mm filaments number 20 and the density (kg/m^3) (a) 420, (b) 397, and (c) 345 from a cross-section view (Continued).

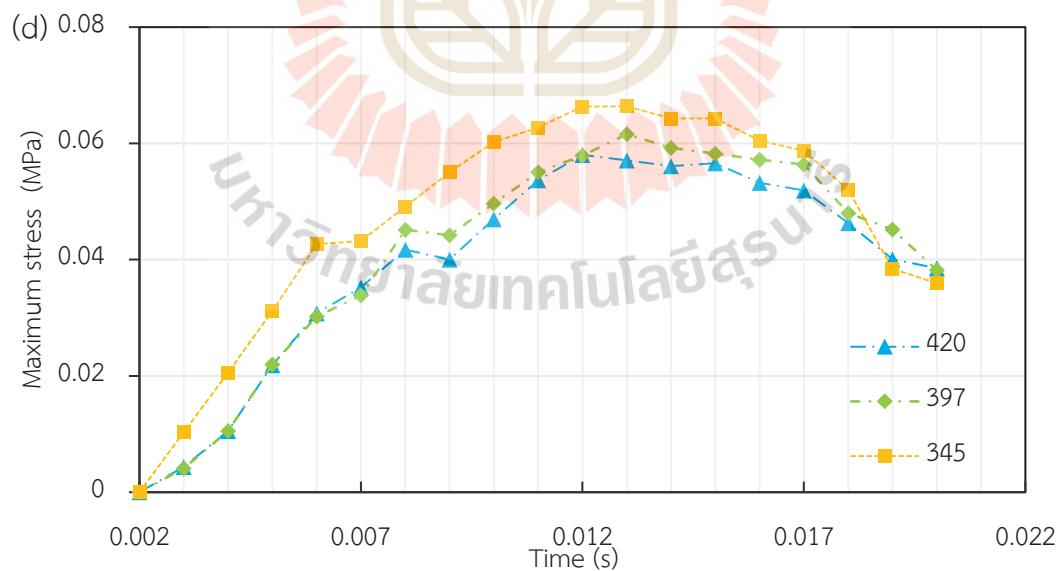


Figure 4.18 d) Maximum stress (MPa) Time (s) plot for the model of filaments number 20 of and the density (kg/m^3) 420, 397, and 345.

filaments number 15.

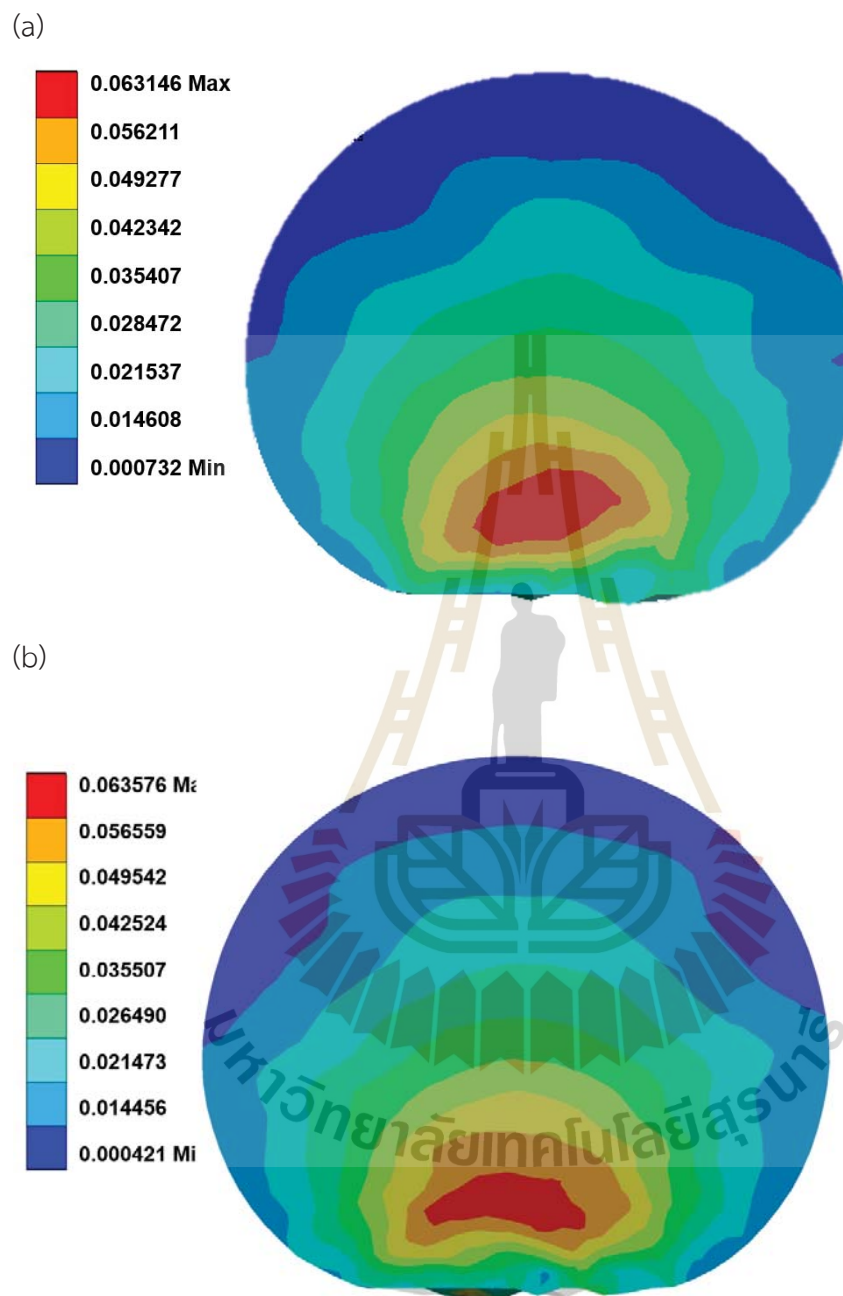


Figure 4.19 Stress [MPa] in the gravity direction for the drop height 100 mm filaments number 15 and the density (kg/m^3) a) 420, and b) 397 from a cross-section view

(c)

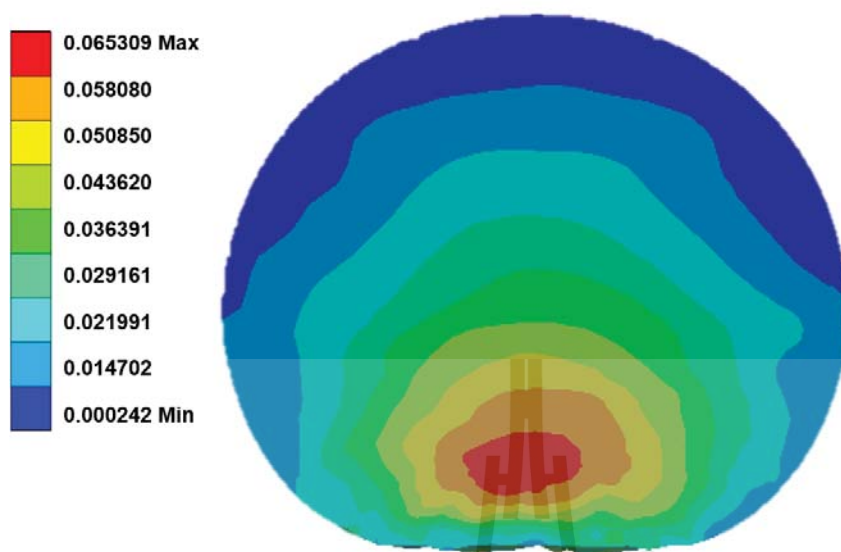


Figure 4.20 Stress [MPa] in the gravity direction for the drop height 100 mm filaments number 15 and the density (kg/m^3) c) 345 from a cross-section view (Continued).



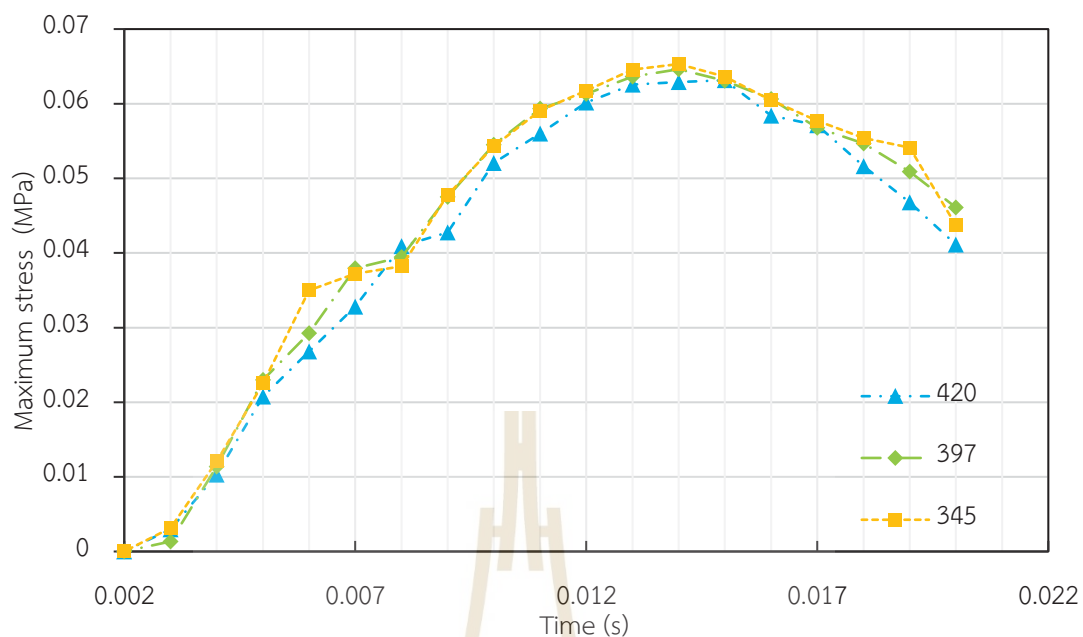


Figure 4.21 Maximum stress (MPa) Time (s) plot for the model of filaments number 15 of and the density (kg/m^3) 420, 397, and 345.

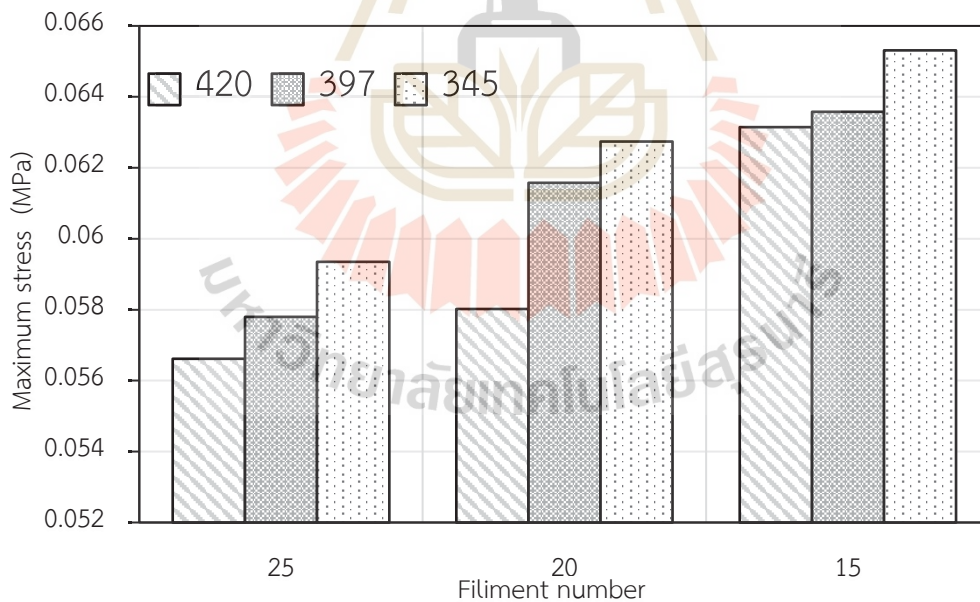
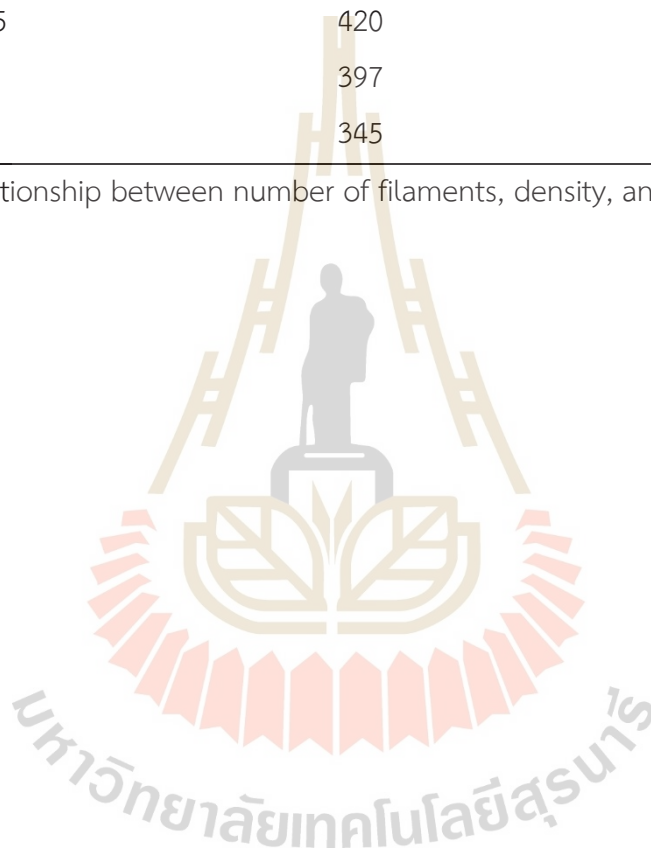


Figure 4.22 Maximum stress values for samples with filament numbers 15, 20, and 25, and densities of 420, 397, and 345 kg/m^3 drop test 100 mm was observed at 0.013 s after impact.

Filaments number	Density (kg/m ³)	Weight (grams)
25	420	20.0271
	397	18.972
	345	16.487
20	420	18.068
	397	17.078
	345	14.841
15	420	15.169
	397	14.338
	345	12.460

Tabel 4.1 Relationship between number of filaments, density, and weight



CHAPTER V

CONCLUSIONS

5.1 Conclusion

This research presented a conceptual design for comprehensive protection of fragile and sensitive agricultural products, particularly fresh fruits, against mechanical damage during transportation and delivery processes. Guava, selected as an exemplary of sensitive agricultural produce, was subjected to foam net drop testing using finite element method (FEM) analysis. The methodology integrated computer-aided design modeling through SolidWorks with analytical simulations performed via ANSYS software for drop test evaluation. Results demonstrated the successful application of finite element analysis in modeling fruit behavior under impact conditions and effectively evaluated critical design parameters (specifically size and number of filaments) in cushion net foam packaging systems. The analysis revealed significant correlations between these design variables and stress distribution patterns within the guava specimens, providing quantitative insight into protective packaging optimization for sensitive agricultural products.

The drop test conducted from a height of 200 mm was used to evaluate the effectiveness of different filament diameters (2.5, 3.5, and 4.5 mm) in reducing the maximum equivalent stress exerted on guava during impact. The unprotected sample exhibited the highest stress at 0.0821 MPa. When a 2.5 mm filament was used, the stress decreased to 0.0728 MPa, with a reduction of approximately 11.32%. Increasing the filament thickness to 3.5 mm further reduced the stress to 0.0696 MPa (15.22% reduction), and the 4.5 mm filament achieved the greatest reduction to 0.0670 MPa, representing an 18.39% decrease.

Impact of filament size, number, and density on cushioning performance

This study demonstrated that filament diameter, filament number, and foam density significantly affect the impact protection performance of the NRLF cushion net for guava. Thicker filaments, particularly the 4.5 mm variant, exhibited superior energy absorption capabilities, effectively reducing the maximum equivalent stress experienced by the fruit during impact. Therefore, increasing filament diameter was recommended to enhance cushioning performance during handling and transportation.

Regarding filament number and density, a consistent trend was observed where reducing either parameter led to an increase in maximum stress values across all tested densities (420, 397, and 345 kg/m³). For instance, at 420 kg/m³, the maximum stress increased from 0.0566 MPa (25 filaments) to 0.0635 MPa (15 filaments), reflecting an approximate 12.19% rise. Similar increases were found for 397 kg/m³ (10.73%) and 345 kg/m³ (9.93%). Comparing across densities at a fixed filament number, reducing the foam density from 420 kg/m³ to 345 kg/m³ at 25 filaments resulted in a 4.95% increase in maximum stress. These findings confirm an inverse relationship between material density and cushioning efficiency.

Overall, these results illustrate a clear engineering trade-off between weight reduction and protective performance. While decreasing foam density and filament quantity contributes to lighter, more material-efficient designs, it also compromises impact resistance, leading to higher stress transmission to the fruit. Furthermore, peak stress was consistently observed approximately 0.013 seconds after impact, underscoring the importance of early-stage energy absorption in cushioning system design.

Maintaining adequate filament thickness, sufficient filament numbers, and appropriate material density are thus essential strategies for achieving an optimal balance between lightweight packaging and reliable protection, supporting the development of sustainable, bio-based packaging solutions.

5.2 Suggestions

The findings of this study provide a foundation for continued research in protective packaging for fragile agricultural products. The following recommendations are proposed for future investigations:

1. Multi-layered Cushion Designs: Explore the effectiveness of composite foam net structures incorporating varied filament thicknesses and density gradients to optimize energy absorption while maintaining lightweight properties.
2. Material Innovation: Investigate alternative bio-based and biodegradable materials with comparable or enhanced mechanical performance relative to natural rubber latex foam (NRLF) to improve environmental sustainability and address resource constraints.
3. Dynamic Real-world Testing: Complement simulation data with experimental validation through physical drop testing under authentic transportation conditions to verify the reliability, durability, and performance of the proposed protective designs.
4. Fruit Variety Application: Extend the established methodology to diverse sensitive horticultural products (e.g., mangoes, tomatoes, berries) to develop customized cushioning solutions based on specific morphological characteristics and mechanical properties.
5. Experimental Validation: While computational modeling provides valuable insights, physical prototype testing through standardized drop tests would validate simulation results and facilitate practical implementation in commercial settings.
6. Extended Impact Scenarios: Future investigations should incorporate diverse impact conditions, including variable drop heights (300-1000 mm), multiple impact angles (0-90°), and sequential impact events to more accurately represent real-world transportation environments.

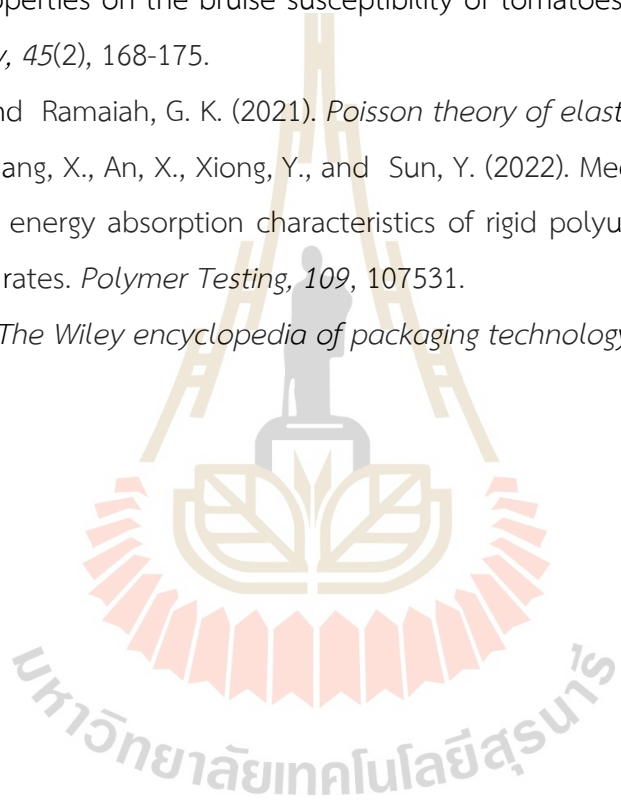
7. Alternative Geometric Configurations: Systematic evaluation of varied cushion net architectures—such as hexagonal arrangements and cross-linked filament patterns—could potentially enhance energy dispersion characteristics and structural adaptability.
8. Hybrid Material Systems: Integration of natural rubber latex foam with complementary eco-friendly materials (e.g., starch-based composites, PLA derivatives) warrants investigation to develop multi-functional cushioning systems offering optimized mechanical performance with enhanced biodegradability.
9. Post-harvest Quality Assessment: Comprehensive analysis of cushioning material effects on fruit quality parameters during extended storage periods should examine critical factors including respiratory gas exchange, moisture retention, and tissue damage metrics.
10. Economic Feasibility Analysis: Rigorous cost-benefit assessment comparing conventional packaging solutions with NRLF-based systems is essential to determine commercial viability and adoption potential across agricultural supply chains.

These strategic research directions build upon current findings and support the development of sustainable, scalable protective packaging innovations for global agricultural distribution networks.

REFERENCES

- Al-Dairi, M., Pathare, P. B., Al-Yahyai, R., and Opara, U. L. (2022). Mechanical damage of fresh produce in postharvest transportation: Current status and future prospects. *Trends in Food Science & Technology*, 124, 195-207.
- Batt, G. S., Lussier, M., Cooksey, K., and Northcutt, J. (2019). Transportation, handling, and microbial growth performance of molded fiber and expanded polystyrene apple trays. *Packaging Technology and Science*, 32(1), 49-56.
- Blackley, D. (1997). *Polymer latices: science and technology. Volume 1: fundamental principles*: Springer.
- Chang, K. (2013). *Product performance evaluation using cad/cae: The computer aided engineering design series*.
- Eaves, D. (2004). *Handbook of polymer foams*: iSmithers Rapra Publishing.
- Gere, J. M., and Timoshenko, S. (1997). *Mechanics of Materials*, ed. Boston, MA: PWS.
- Goodwin, D., and Young, D. (2011). *Protective packaging for distribution: design and development*.
- Hatton, K. O. (1998). *Effect of temperature on shock absorption properties of cushioning materials*: San Jose State University.
- Lin, M., Fawole, O. A., Saeys, W., Wu, D., Wang, J., Opara, U. L., Chen, K. (2023). Mechanical damages and packaging methods along the fresh fruit supply chain: A review. *Critical Reviews in Food Science and Nutrition*, 63(30), 10283-10302.
- Mei, M., Cai, Z., Zhang, X., Sun, C., Zhang, J., Peng, H., Zhang, W. (2023). Early bruising detection of 'Korla' pears by low-cost visible-LED structured-illumination reflectance imaging and feature-based classification models. *Frontiers in Plant Science*, 14, 1324152.
- Sadrehaghghi, I. (2021). Dynamic & Adaptive Meshing. *CFD Open Series, Patch*, 2.
- Saengwong-Ngam, R., Saengrayap, R., Rattanakaran, J., Arwatchananukul, S., Aunsri, N., Tontiwattanakul, K., Kitazawa, H. (2024). Cushion performance of eco-friendly natural rubber latex foam composite with bamboo leaf fiber for impact protection of guava. *Postharvest biology and technology*, 208, 112663.

- Stopa, R., Szyjewicz, D., Komarnicki, P., and Kuta, Ł. (2018). Determining the resistance to mechanical damage of apples under impact loads. *Postharvest biology and technology*, 146, 79-89.
- Truesdell, C. (1976). History of classical mechanics: Part II, the 20th centuries. *Naturwissenschaften*, 63, 119-130.
- Van Zeebroeck, M., Darius, P., De Ketelaere, B., Ramon, H., and Tijskens, E. (2007). The effect of fruit properties on the bruise susceptibility of tomatoes. *Postharvest biology and technology*, 45(2), 168-175.
- Vijayakumar, K., and Ramaiah, G. K. (2021). *Poisson theory of elastic plates*: Springer.
- Xiao, Y., Yin, J., Zhang, X., An, X., Xiong, Y., and Sun, Y. (2022). Mechanical performance and cushioning energy absorption characteristics of rigid polyurethane foam at low and high strain rates. *Polymer Testing*, 109, 107531.
- Yam, K. L. (2010). *The Wiley encyclopedia of packaging technology*: John Wiley & Sons.



BIOGRAPHY

Mr. Theerapat Taweabraksa holds a Bachelor's degree in Polymer Engineering from Suranaree University of Technology and is currently pursuing a Master of Engineering degree in Materials Engineering at the same institution. His strong interest in material science and engineering design, particularly the Finite Element Method (FEM), led him to apply this advanced knowledge to his master's thesis.

His inspiration for the thesis, "DESIGNING OF ECO-FRIENDLY FOAM NET FOR GUAVA USING FINITE ELEMENT METHOD (FEM)", stems from a strong desire to develop sustainable packaging solutions. By using FEM, he can accurately simulate and analyze the behavior of foam materials, allowing for the design of an optimal packaging structure that is both highly protective and minimizes material usage. This approach aligns with his core mission: to create innovative, environmentally friendly solutions for a more sustainable world.

มหาวิทยาลัยเทคโนโลยีสุรนารี